Molecular Vision 2020; 26:797-817 <http://www.molvis.org/molvis/v26/797>
Received 31 March 2020 | Accepted 28 December 2020 | Published 30 December 2020

Osmotic regulation of aquaporin-8 expression in retinal pigment epithelial cells in vitro: Dependence on K_{ATP} channel activation

Benjamin Schnabel,[1] Heidrun Kuhrt,[2] Peter Wiedemann,[1] Andreas Bringmann,[1] Margrit Hollborn[1]

[1]Department of Ophthalmology and Eye Hospital, University of Leipzig, Leipzig, Germany; [2]Institute of Anatomy, Medical Faculty, University of Leipzig, Germany

Purpose: The expression of aquaporin-8 (*AQP8*), which plays a crucial role in the maintenance of the cellular fluid and electrolyte balance, was shown to be increased in RPE cells under hyperosmotic conditions. The aim of the present study was to investigate the mechanisms of hyperosmotic *AQP8* gene expression and the localization of AQP8 in cultured human RPE cells.

Methods: Hyperosmolarity was produced with the addition of 100 mM NaCl or 200 mM sucrose. Hypoxia was induced by cell culture in a 0.2% O_2 atmosphere or the addition of the hypoxia mimetic $CoCl_2$. Oxidative stress was induced by the addition of H_2O_2. Gene expression was determined with real-time RT–PCR analysis. AQP8 protein localization and secretion of VEGF were evaluated with immunocytochemistry, western blotting, and enzyme-linked immunosorbent assay (ELISA).

Results: Immunocytochemical and western blot data suggest that the AQP8 protein is mainly located in the mitochondria. Extracellular hyperosmolarity, hypoxia, and oxidative stress induced increases in *AQP8* gene expression. Hyperosmotic *AQP8* gene expression was reduced by inhibitors of the p38 MAPK and PI3K signal transduction pathways, and by JAK2 and PLA_2 inhibitors, and was in part mediated by the transcriptional activity of CREB. Hyperosmotic *AQP8* gene expression was also reduced by autocrine/paracrine interleukin-1 signaling, the sulfonylureas glibenclamide and glipizide, which are known inhibitors of K_{ATP} channel activation, and a pannexin-blocking peptide. The K_{ATP} channel opener pinacidil increased the expression of *AQP8* under control conditions. The cells contained *Kir6.1* and *SUR2B* gene transcripts and displayed Kir6.1 immunoreactivity. siRNA-mediated knockdown of *AQP8* caused increases in hypoxic VEGF gene expression and secretion and decreased cell viability under control, hyperosmotic, and hypoxic conditions.

Conclusions: The data indicate that hyperosmotic expression of *AQP8* in RPE cells is dependent on the activation of K_{ATP} channels. The data suggest that AQP8 activity decreases the hypoxic VEGF expression and improves the viability of RPE cells which may have impact for ischemic retinal diseases like diabetic retinopathy and age-related macular degeneration.

Development of retinal edema is an important complication of various vision-threatening diseases, including exudative (neovascular) age-related macular degeneration (AMD) and diabetic retinopathy [1,2]. Edema is characterized by water accumulation in retinal tissue. In exudative AMD, fluid accumulation occurs in the subretinal space resulting in functional impairment of photoreceptors and serous retinal detachment. Water accumulation within retinal tissue results from an imbalance between the water influx from the blood into the retina and water clearance from retinal tissue into the blood [3]. Normally, fluid absorption from retinal tissue is mainly mediated by the coupled transport of osmolytes (in particular, of potassium and chloride ions) and water through glial and RPE cells [3-6]. The transcellular water transport is facilitated by aquaporin (AQP) water channels. Thirteen members of the AQP protein family (AQP0–12) were identified in mammals which mediate bidirectional movement of water across membranes in response to osmotic gradients and differences in hydrostatic pressure. Various AQP subtypes also mediate the transmembrane transport of small noncharged solutes, such as glycerol, lactate, urea, ammonia, and H_2O_2 [7]. Facilitated water transport is important for the permission of rapid ion currents and the resolution of osmotic gradients within tissues and across membranes; the latter is important for the integrity and volumes of cells and mitochondria. Human RPE cells were reported to express gene transcripts of various AQP subtypes, including AQP1, AQP3, AQP5, and AQP8 [5,8-10].

Osmotic gradients between the blood and retinal tissue, and between intra- and extracellular compartments, contribute to the development of retinal edema [11]. Hyperglycemia, which increases extracellular osmolarity [12], is the primary risk factor, and systemic hypertension is the main secondary risk factor of diabetic retinopathy [13,14]. In addition, the increased glucose flux through the polyol pathway produces intracellular sorbitol accumulation and increased intracellular osmotic pressure [15]. Hypertension is also a

Correspondence to: Margrit Hollborn, Department of Ophthalmology and Eye Hospital, University of Leipzig, Faculty of Medicine, Liebigstrasse 10-14, D-04103 Leipzig, Germany; Phone: +49 (0) 341 97 21 561; FAX: +49(0) 341 97 21 659; email: hollbm@medizin.uni-leipzig.de

risk factor of AMD [16,17]. The main condition that causes acute hypertension is increased extracellular osmolarity following intake of dietary salt (NaCl) [18]. In experimental diabetic retinopathy, the expression of retinal AQPs is altered [19,20]; high salt intake aggravates the diabetic alterations of retinal AQP expression independently from changes in blood pressure [21]. It was shown that extracellular hyperosmolarity induces the expression of *AQP3* (Gene ID: 360; OMIM: 600170), *AQP5* (Gene ID: 362; OMIM: 600442), and *AQP8* (Gene ID: 343; OMIM: 603750) genes in human RPE cells [8,10]. Expression of the *AQP5* gene in RPE cells was found to be regulated by extracellular osmolarity, with up- and downregulation in response to hyper- and hypo-osmotic conditions, respectively [10]. However, the mechanisms of hyperosmotic *AQP8* gene expression in RPE cells was not investigated until today. In various cell types, AQP8 is localized to the plasma membrane, intracellular vesicles, or inner mitochondrial membrane [22–24]. Upon stimulation, AQP8 localized to secretory vesicles is inserted into the plasma membrane to increase the osmotic water and H_2O_2 membrane permeability [25]. H_2O_2 plays a key role in the regulation of tyrosine phosphatase and kinase signaling induced, for example, by activation of growth factor receptors, like vascular endothelial growth factor (VEGF) receptors [26,27]. AQP8 localized to the inner mitochondrial membrane facilitates the efflux of metabolic water, which is a byproduct of adenosine 5′-triphosphate (ATP) synthesis, thus preventing mitochondrial swelling [23,24]. AQP8 in mitochondria also facilitates the transmembrane diffusion of solutes like H_2O_2 [28,29] and ammonia/ammonium, and thus, contributes to maintenance of the acid-base equilibrium, regulation of the cellular and mitochondrial oxidative stress levels, and detoxification of ammonia via mitochondrial urea synthesis [30-32]. However, the subcellular localization of AQP8 in RPE cells is unknown. The present study was performed to investigate in cultured human RPE cells the subcellular localization of AQP8 and the cellular mechanisms of hyperosmotic *AQP8* expression, and to investigate whether knockdown of *AQP8* has effects on three important physiologic properties of RPE cells implicated in retinal diseases in situ: cell proliferation and viability, and expression and secretion of VEGF. Because we found that hypoxia induces delayed expression of the *AQP8* gene, we investigated the effects of *AQP8* knockdown under hyperosmotic and hypoxic conditions. We also found that inhibition of the activation of ATP-sensitive potassium (K_{ATP}) channels reduces hyperosmotic *AQP8* gene expression; therefore, we investigated the expression of *Kir6.1* (Gene ID: 3764; OMIM: 600935) and *Kir6.2* (Gene ID: 3767; OMIM: 600937) in the cells.

METHODS

Human material: The use of human material was approved by the Ethics Committee of the University of Leipzig (#745, 07/25/2011) and was performed according to the Declaration of Helsinki. Postmortem eyes from human cornea donors without reported eye disease were obtained within 48 h of death; written informed consent for the use of retinal tissue in basic science was obtained from the relatives of each donor.

Materials: Human recombinant interleukin-1β (IL-1β), IL-1 receptor antagonist, platelet-derived growth factor-BB (PDGF), transforming growth factor-β1 (TGF-β1), and VEGF-A_{165} were purchased from R&D Systems (Abingdon, UK). The following compounds were obtained from Calbiochem (Bad Soden, Germany): AG490, 8-(3-chlorostyryl) caffeine (CSC), 8-cyclopentyl-1,3-dipropylxanthine (DPCPX), Gö6976, H-89, and U73122. Dithiothreitol was from Carl Roth (Karlsruhe, Germany), and PD173074 was kindly provided by Pfizer (Karlsruhe, Germany). 666–15, A-438079, AR-C 118925XX, caffeic acid phenethyl ester (CAPE), cyclosporin A, GSK650394, the hypoxia-inducible transcription factor (HIF)-1 inhibitor, LY294002, human recombinant matrix metalloproteinase-2 (purified active form), MRS2179, NS-398, the pannexin-blocking peptide ^{10}panx, the scrambled control peptide ^{10}panxScr, PD98059, PP2, SB203580, SP600125, SR11302, and SU1498 were purchased from Tocris (Ellisville, MO). Ac-YVAD-CMK, AG1478, and Stattic were from Enzo Life Science (Lausen, Switzerland). MCC950 was from InvivoGen (San Diego, CA). 4’,6-Diamidin-2-phenylindol (DAPI) was from Invitrogen (Paisley, UK). Human-specific small interfering RNA (siRNA) against nuclear factor of activated T cell 5 (NFAT5) and AQP8, respectively, and nontargeted control siRNA were obtained from Santa Cruz Biotechnology (Heidelberg, Germany). N-acetyl-L-cysteine, acetylsalicylic acid, AG1296, arachidonic acid, bis-(o-aminophenoxy)ethane-*N*,*N*,*N*′,*N*′-tetra-acetic acid acetoxymethyl ester (BAPTA/AM), 4-bromophenacyl bromide, carbenoxolone, glibenclamide, glipizide, ibuprofen, indomethacin, PD150606, 1,10-phenanthroline, pinacidil, probenecide, prostaglandin E_2, ruthenium red, SB431542, suramin, triamcinolone acetonide, VU0285655–1, VU0359595, and all other substances used were from Sigma-Aldrich (Taufkirchen, Germany), unless stated otherwise.

Cell culture: Preparation and culture of the RPE cells were described previously [33]. Cell lines of passages 3–5 were used; each line was used in three to ten different experiments. Cells that achieved a confluency of about 90% were cultured in serum-free medium for 16 h. During this period, the cultures reached 100% confluency. Thereafter, test

substances were added to the serum-free medium. Extracellular hyperosmolarity was produced with the addition of NaCl or sucrose to the medium. Extracellular hypo-osmolarity (60% of control osmolarity) was produced with the addition of distilled water. Hypoxia was induced with the addition of the hypoxia mimetic $CoCl_2$ (150 µM) [34] or with cell culture in a 0.2% O_2 atmosphere. Inhibitory agents were preincubated for 30 min.

RNA extraction and cDNA synthesis: Total RNA was extracted with the InviTrap Spin Universal RNA Mini Kit (Stratec Molecular, Berlin, Germany). The A_{260}/A_{280} ratio of the optical density of the RNA samples (measured with NanoDrop1000; peQLab, Erlangen, Germany) was between 1.95 and 2.05, indicating adequate RNA quality. After treatment with DNase I (Roche, Mannheim, Germany), cDNA was synthesized from 0.5 µg RNA with a reverse transcription kit (ThermoFisher Scientific, Waltham, MA).

RT–PCR analysis: RT–PCR was performed with the Taq PCR Master Mix kit (Qiagen, Hilden, Germany) and the primer pairs described in Table 1. One microliter of the first-strand mixture and 0.25 µM of each gene-specific sense and antisense primers were used for amplification in a final volume of 20 µl. Amplification was performed for 40 cycles with the PTC-200 Thermal Cycler (MJ Research, Watertown, MA). Each cycle consisted of 30 s at 94 °C, 60 s at 58 °C, and 1 min at 72 °C.

Real-time RT–PCR analysis: Semiquantitative real-time RT–PCR analysis was performed with the CFX Connect Real-Time PCR Detection System (BioRad, Munich, Germany) and the primer pairs described in Table 1. The amplification

Table 1. Primer pairs used in PCR experiments.

Gene / Accession number	Gene ID/ OMIM	Primer sequence (5′→3′)	Product (bp)
ACTB [a, b] NM_001101	60/ 102630	F: ATGGCCACGGCTGCTTCCAGC R: CATGGTGGTGCCGCCAGACAG	237
AQP8 [a] NM_001169.2	343/ 603750	F: TCCTGAGGAGAGGTTCTGGA R: AGGGCCCTTTGTCTTCTCAT	157
AQP8 [b] NM_001169.2		F: AGCCTGAATTTGGCAATGAC R: AGTGTCCGTCCCATTCTCAAT	164
KIR6.1 [b] NM_004982.3	3764/ 600935	F: GGAGGGAGGATGATGACAGA R: TTTCCTCAGGTCACCCACTC	222
KIR6.2 [b] NM_000525.3	3767/ 600937	F: ATCATCGTCATCCTGGAAGG R: GGTGTTGCCAAACTTGGAG	162
SUR1 [b] NM_001351297.1	6833/ 600509	F: TACACAGACTCCAACAACATTGC R: GAGACCATTAGGGCGTAGGTAAG	188
SUR2A [b] NM_005691.3	10060/ 601439	F: TAGTAATGACAGCCTTTGCAGAC R: GTCATCACCAAAGTGGAAAAGAG	172
SUR2B [b] NM_020297		F: TAGTAATGACAGCCTTTGCAGAC R: GCGAACAAAAGAAGCAAATACTC	170
CYP11B1 [b] NM_000497.3	1584/ 610613	F: TACACCAGACCTTCCAGGAACTA R: AGCAAGAACACGCCACATTT	193
CYP11B2 [b] NM_000498.3	1585/ 124080	F: CTTGGTGCTTCAGAACTACCACA R: TTAGTGTCTCCACCAGGAAGTGC	263
NFAT5 [b] NM_006599.3	10725/ 604708	F: TCACCATCATCTTCCCACCT R: CTGCAATAGTGCATCGCTGT	174
VEGFA$_{188, 164, 120}$ [b] NM_003376.5 NM_001287044.1 NM_001025370.2	7422/ 192240	F: CCTGGTGGACATCTTCCAGGAGTA R: CTCACCGCCTCGGCTTGTCACA	479, 407, 275

[a],used in RT–PCR analysis.[b],used in real-time RT–PCR analysis.

reaction mixture (15 µl) consisted of 7.5 µl of 2×iQ SYBR Green Supermix (BioRad), the specific primer set (0.2 µM each), and 2 µl (2.5 ng for the *AQP8* primer pair) and 1 µl (1.25 ng for the other primer pairs) of cDNA. The following conditions were used: one cycle of denaturation at 95 °C for 3 min, 45 cycles of denaturation at 95 °C for 30 s, annealing at 60 °C (*AQP8*) and at 58 °C for 20 s, extension at 72 °C for 45 s, and a melting curve at 55 °C with the temperature gradually increased for 0.5 °C up to 95 °C. The correct lengths of the PCR products were proved with agarose gel electrophoresis. mRNA expression levels were normalized to the level of β-actin (*ACTB,* Gene ID: 60; OMIM: 102630) mRNA. Changes in mRNA expression were calculated according to the $2^{-\Delta\Delta CT}$ method [35].

siRNA transfection: Cells were seeded at 7×10^4 cells per well in 12-well culture plates and were allowed to grow to a confluency of 60–80%. Thereafter, the cells were transfected with NFAT5 siRNA and nontargeted siRNA (5 nM each), respectively, using HiPerfect reagent (Qiagen) in F-10 medium containing 10% fetal bovine serum (FBS; Invitrogen) according to the manufacturer's instructions. After 48 h (a time point at which the cultures were confluent), NaCl (100 mM) was added for a further 6 h. Total RNA was extracted, and the *AQP8* mRNA level was determined with real-time RT–PCR. To knock down *AQP8*, the cells were cultured for 24 h (the time point of the strongest knockdown) in F-10 medium containing 10% FBS, transfection reagent, and AQP8 siRNA and nontargeted siRNA (10 nM each). Then, the cells were cultured in serum-free medium in the absence (6 and 24 h) and presence of high (+ 100 mM) NaCl (6 h) and $CoCl_2$ (150 µM; 24 h), respectively, or in a 0.2% O_2 atmosphere (24 h).

Western blot analysis: The cells were seeded at 5×10^5 cells per well in six-well plates and were cultured in FBS (10%)-containing F-10 medium. When a confluency of 80–90% was achieved, the cells were growth arrested for 12 h in serum-free medium. After the medium was removed, the cells were washed twice with prechilled PBS (1X; 155 mM NaCl, 1.54 mM KH_2PO_4, 2.71 mM Na_2HPO_4-$7H_2O$ pH 7.2; Invitrogen) and scraped into 180 µl of lysis buffer (50 mM Tris-HCl, pH 8.0, 5 mM EDTA, 150 mM NaCl, 0.5% NP-40, 1% protease inhibitor cocktail, 1% phosphatase inhibitor cocktail). The cell lysates were centrifuged at 20,124 ×*g* for 10 min. Equal amounts of cytosolic protein (50 µg) were separated with 12.5% sodium dodecyl sulfate–polyacrylamide gel electrophoresis (SDS–PAGE). Immunoreactive bands were probed with primary and secondary antibodies, and visualized using 5-bromo-4-chloro-3-indolyl phosphate/nitro blue tetrazolium. The antibodies used are described in Table 2.

Immunocytochemistry: The cultures were fixed with 1% paraformaldehyde for 20 min on ice. After several washing steps in prechilled PBS (pH 7.4; Invitrogen), the cultures were incubated in PBS containing 0.3% Triton X-100 for 15 min at room temperature. Blocking of nonspecific antibody binding was performed with PBS containing 10% normal goat serum and 0.3% Triton X-100 for 2 h at room temperature. Primary antibodies diluted in blocking solution were incubated at 4 °C overnight. After several washing steps in PBS plus 0.3% Triton X-100, the secondary antibody was applied for 2 h at room temperature. After additional washing steps, DAPI (1:10,000) was added for 15 min at room temperature. The coverslips were mounted with Fluorescence Mounting Medium (DakoCytomation, Glostrup, Denmark). Images were taken with an epifluorescence microscope (Olympus BX40, Olympus, Essex, UK), a charge-coupled device (CCD) camera (Olympus XM10), and cellSens software (Olympus). The antibodies used are described in Table 2.

Preparation of RPE sections: A human donor eye was fixed in 4% paraformaldehyde at pH 7.4 for 4 days. The penetration of the fixative was improved with a small incision in the sclera of the eye. To prepare the paraffin sections, the eye was passed through an ascending series of alcohol, incubated in organic solutions, and embedded in Histowax (Histolab Products, Gothenburg, Sweden) according to a common protocol [36]. Ten-micrometer-thick sections were cut with a rotation microtome (HM 355S; ThermoFisher Scientific).

Immunohistochemistry: After deparaffinization, the sections were pretreated with 0.01 M citrate buffer, pH 6.0, in a microwave oven for 2 × 20 min at 96 °C to achieve antigen retrieval. Nonspecific binding sites were blocked with PBS containing 5% normal goat serum plus 0.3% Triton X-100 for 2 h at room temperature. Primary antibodies diluted in blocking solution were incubated at 4 °C overnight. After washing in PBS plus 0.3% Triton X-100, secondary antibodies were applied for 2 h at room temperature. Following several washing steps with PBS, the cell nuclei were labeled with DAPI for 15 min at room temperature. The sections were mounted with Fluorescence Mounting Medium (DakoCytomation). The antibodies used are described in Table 2.

ELISA, cell proliferation, and cell viability assays: After transfection of AQP8 siRNA and nontargeted siRNA (10 nM each), respectively, the cells were cultured for 24 h in serum-free medium or in the cell proliferation assay, a medium that contained 0.5% serum, in the absence and presence of high (+ 100 mM) NaCl and $CoCl_2$ (150 µM), respectively, or in a 0.2% O_2 atmosphere. The level of VEGF-A_{165} in the cultured media (100 µl) was determined with enzyme-linked immunosorbent assay (ELISA; R&D Systems). Bromodeoxyuridine

Table 2. Antibodies used in immunocytochemistry (ICC), immunohistochemistry (IHC), and western blot (WB) analysis.

Method	Antibody	Source	Catalog #	Dilution Concentration
ICC	rabbit anti-human AQP8	antibodies-online, Aachen, Germany	ABIN571717	1:500 2 µg/ml
	rabbit anti-human Kir6.1	Invitrogen, Paisley, UK	ThermoFisher Scientific, Waltham, MA – PA5–56628	1:200 0.5 µg/ml
	monoclonal mouse anti-human cytochrome c	Santa Cruz Biotechnology, Heidelberg, Germany	ThermoFisher Scientific – sc13156	1:50 4 µg/ml
	monoclonal mouse anti-human ZO-1	Invitrogen	33–9100	1:100 5 µg/ml
	Cy3-coupled goat anti-rabbit IgG	Jackson Immuno Research, West Grove, PA	111–165–003	1:200 10 µg/ml
	Alexa Fluor 488-coupled goat anti-mouse IgG	Invitrogen	ThermoFisher Scientific – A-11001	1:200 10 µg/ml
IHC	rabbit anti-human AQP8	antibodies-online	ABIN571717	1:500 2 µg/ml
	monoclonal mouse anti-human ZO-1	Invitrogen	33–9100	1:50 10 µg/ml
	monoclonal mouse anti-human cytochrome c	Santa Cruz Biotechnology	sc13156	1:50 4 µg/ml
	Alexa 568-coupled goat anti-rabbit IgG	Invitrogen	A11036	1:400 5 µg/ml
	Alexa 647-coupled goat anti-mouse IgG	Invitrogen	A21236	1:200 10 µg/ml
WB	rabbit anti-human AQP8	antibodies-online	ABIN571717	1:1000 1 µg/ml
	rabbit anti-β-actin	Cell Signaling Technology, Frankfurt/M., Germany	4970	1:1000 37 ng/ml
	alkaline phosphatase-linked anti-rabbit IgG	Cell Signaling Technology	7054S	1:2000 35.5 ng/ml

(BrdU) incorporation as a marker of the cell proliferation rate was determined with the Cell Proliferation ELISA BrdU Kit (Roche). BrdU (10 µM) was added to the culture medium 5 h before fixation. Cell viability was determined with a 3-(4,5-dimethylthiazol-2-yl)-2,5-diphenyltetrazolium bromide (MTT) assay (Serva, Heidelberg, Germany). Ten microliters of MTT solution (5 mg/ml) were added to each well after a 20-h period of stimulation. After 4 h, the culture supernatants were removed, and dimethyl sulfoxide (DMSO; 100 µl) was added. Absorbance was recorded at 570 nm with the Spectra Max 50 ELISA reader (Molecular Devices, Sunnyvale, CA).

Statistical analysis: At least three independent experiments with cell lines from different donors were performed for each test. Data are shown as means ± standard error of the mean (SEM). Statistical analysis was performed with Prism (GraphPad Software, San Diego, CA). Significant differences were evaluated with one-way analysis of variance (ANOVA), the Bonferroni multiple comparison post hoc test, and the Mann–Whitney U test. A p value of less than 0.05 was considered statistically significant.

RESULTS

Regulation of AQP8 gene expression: As previously described [8-10], the cultured human RPE cells contained *AQP8* gene transcripts (Figure 1A). Real-time RT–PCR analysis was performed to investigate whether alterations in the extracellular osmolarity induce changes in *AQP8* gene expression in RPE cells. As shown in Figure 1B, expression of the *AQP8* gene was statistically significantly ($p<0.05$) increased when the cells were cultured for 2 and 6 h in media that were made hyperosmotic by the addition of either 100 mM NaCl or 200 mM sucrose (both induce equal increases in extracellular osmolarity). Coaddition of NaCl and sucrose did not cause an additive increase in *AQP8* gene expression after 2 h of stimulation (Figure 1B). There was a statistically

significant difference ($p<0.05$) between the *AQP8* expression levels induced by high NaCl and sucrose after 6 h of stimulation (Figure 1B). Although the hyperosmotic expression of *AQP8* gene expression attenuated to the control level after 24 h of treatment with high NaCl or sucrose, coaddition of NaCl and sucrose induced a statistically significant ($p<0.05$) increase in *AQP8* gene expression also after 24 h of treatment (Figure 1B). NaCl-induced expression of the *AQP8* gene was dose-dependent; statistically significant ($p<0.05$) increases in the level of the *AQP8* transcripts were found when more than 10 mM NaCl was added to the medium (Figure 1C). A hypo-osmotic medium (60% of control osmolarity) induced biphasic regulation of *AQP8* gene expression, with downregulation and upregulation after 6 and 24 h of stimulation, respectively (Figure 1D).

Chemical hypoxia induced with the addition of $CoCl_2$ (150 µM) to the culture medium [34] caused upregulation of *AQP8* gene expression after 24 h of stimulation, while cell culture in a 0.2% O_2 atmosphere caused time-dependent expression of the *AQP8* gene (Figure 1E). Oxidative stress induced with the addition of H_2O_2 (20 µM) induced a transient increase in the level of the *AQP8* transcripts after 6 h of stimulation (Figure 1E). In agreement with a previous study [9], cell culture in a high (25 mM) glucose medium was associated with a decrease in *AQP8* gene expression after 2 h of stimulation (Figure 1F). Addition of the anti-inflammatory glucocorticoid triamcinolone acetonide to the culture medium induced a statistically significant ($p<0.05$) increase in the cellular level of the *AQP8* transcripts after 6 and 24 h of stimulation, whereas addition of VEGF induced downregulation of *AQP8* gene expression after 24 h of stimulation (Figure 1F). The following agents had no statistically significant ($p>0.05$) effects on *AQP8* gene expression within 24 h of stimulation in iso-osmotic medium (data not shown): PDGF (10 ng/ml), TGF-β1 (10 ng/ml), IL-1β (10 ng/ml), prostaglandin E_2 (10 ng/ml), and matrix metalloproteinase-2 (10 ng/ml). In agreement with a previous study [8], arachidonic acid (5 µM) and fetal calf serum (10%) also had no effects on *AQP8* gene expression (data not shown). The data indicate that expression of the *AQP8* gene in RPE cells is induced by extracellular hyperosmolarity, hypoxia, and oxidative stress.

Subcellular localization of AQP8: It was shown in various cell types that the non-glycosylated type of AQP8 (with a molecular weight of about 27 kDa) is mainly expressed in the inner mitochondrial membrane, while glycosylated types of AQP8 (with molecular weights between 30 and 38 kDa) are predominantly localized to the plasma membrane [23,24,37]. To determine whether RPE cells contain non-glycosylated and/or glycosylated types of AQP8, we performed western blotting. As shown in Figure 2A, the AQP8 protein was found in different bands, e.g., around 27 and 37 kDa, suggesting that cultured RPE cells contain non-glycosylated and glycosylated types of AQP8. The different densities of the bands may suggest a higher expression level of AQP8 in mitochondria than in the plasma membrane.

We immunostained RPE cell cultures and an RPE monolayer that was freshly isolated from a donor eye with antibodies against AQP8, the mitochondrial marker cytochrome c, and the plasma membrane protein zonula occludens-1 (ZO-1; also known as tight junction protein-1). In the RPE cell cultures, AQP8 immunoreactivity partially colocalized with the cytochrome c immunoreactivity (Figure 2B). The RPE cell cultures were also labeled with the anti-ZO-1 antibody; in various areas, ZO-1 immunoreactivity was arranged in lines at the cell borders (Figure 2C). Cultures that were colabeled with the anti-AQP8 and anti-ZO-1 antibodies showed no colocalization of the two immunoreactivities (Figure 2D). Similarly, there was no colocalization of the two immunoreactivities in the RPE monolayer (Figure 2E). ZO-1 immunoreactivity was arranged in lines around the cells, while AQP8 immunoreactivity was found in spherical structures beside the nuclei within the cells, likely representing mitochondria and/or intracellular vesicles. However, there was colocalization of AQP8 and cytochrome c immunoreactivities in the freshly isolated RPE monolayer (Figure 2F). The data suggest that AQP8 in RPE cells is mainly located in the mitochondria.

Intracellular signaling involved in mediating NaCl-induced AQP8 gene expression: It was shown that high extracellular NaCl induces activation of different signal transduction molecules in RPE cells, e.g., p38 mitogen-activated protein kinase (p38 MAPK) and extracellular signal-regulated kinases 1 and 2 (ERK1/2) [10]. To investigate the intracellular signaling involved in mediating NaCl-induced expression of the *AQP8* gene in RPE cells, we tested pharmacological blockers of various intracellular signal transduction molecules in cultures that were stimulated for 6 h with high (+ 100 mM) NaCl. As shown in Figure 3, the NaCl-induced expression of the *AQP8* gene was statistically significantly ($p<0.05$) decreased in the presence of the following inhibitors: the inhibitor of p38 MAPK activation, SB203580, the inhibitor of phosphatidylinositol-3 kinase (PI3K)-related kinases, LY294002, the Janus kinase 2 (JAK2) inhibitor AG490, and the phospholipase A_2 (PLA_2) inhibitor 4-bromophenacyl bromide. The inhibitor of ERK1/2 activation, PD98059, the c-Jun NH_2-terminal kinase (JNK) inhibitor SP600125, and the inhibitor of the serum and glucocorticoid-regulated kinase, GSK650394, had no effects on the NaCl-induced expression of the *AQP8* gene (Figure 3). The following agents also had

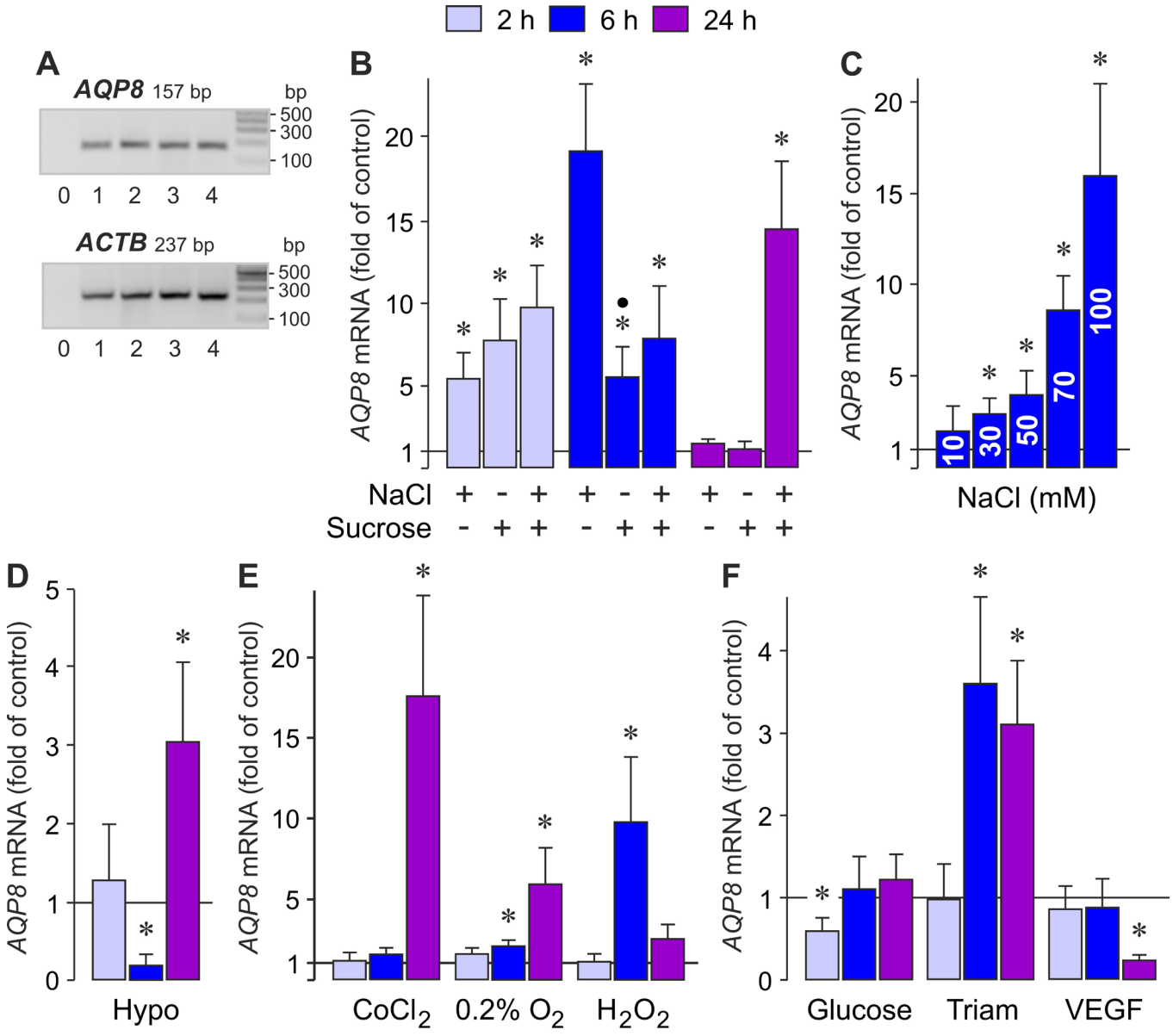

Figure 1. Regulation of *AQP8* gene expression in cultured human RPE cells. **A**: Presence of *AQP8* gene transcripts in RPE cells, as determined with RT–PCR analysis. The correct lengths of the RT–PCR products were confirmed with agarose gel electrophoresis using products obtained from cell lines of four different donors (1–4). Negative controls (0) were performed with double-distilled water instead of cDNA as the template. *ACTB* mRNA was used as loading control. **B**: Effects of media which were made hyperosmotic with the addition of 100 mM NaCl or 200 mM sucrose, or with the coaddition of both agents, on *AQP8* gene expression. The level of *AQP8* mRNA was determined with real-time RT–PCR analysis in cells cultured for 2, 6, and 24 h (as indicated by the panels of the bars), and is expressed as folds of unstimulated control. **C**: Dose-dependency of the effect of high extracellular NaCl on the *AQP8* mRNA level. Ten to 100 mM NaCl were added to the culture medium, as indicated in the bars. **D**: Effect of extracellular hypo-osmolarity (Hypo; 60% osmolarity) on the cellular level of *AQP8* mRNA. **E**: Effects of the hypoxia mimetic $CoCl_2$ (150 µM), cell culture in a 0.2% O_2 atmosphere, and oxidative stress induced by addition of H_2O_2 (20 µM) on expression of the *AQP8* gene. **F**: Effects of high (25 mM) glucose, triamcinolone acetonide (Triam; 50 µM), and exogenous VEGF (10 ng/ml) on *AQP8* gene expression. Each bar represents mean ± standard error of the mean (SEM) obtained in four to ten independent experiments using cell lines from different donors. Significant difference vs. unstimulated control: *p<0.05. Significant difference vs. NaCl and sucrose: •p<0.05.

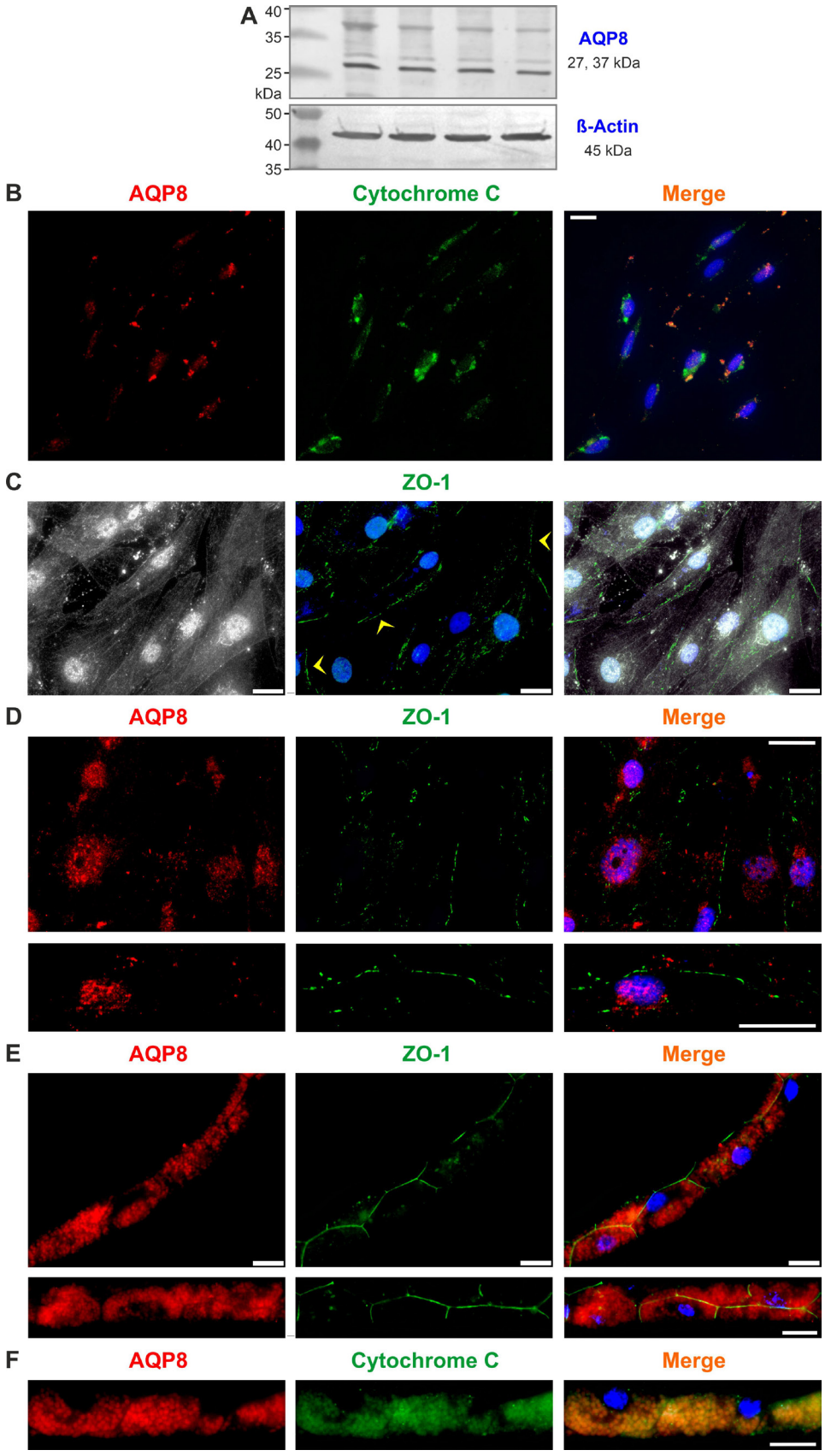

Figure 2. Subcellular localization of the AQP8 protein in human RPE cells. **A**: In western blots of the lysates of cell lines from four different donors, the AQP8 protein was found in different bands, e.g., around 27 and 37 kDa. β-Actin (45 kDa) was used as loading control. **B**: Double immunolabeling of a cell culture with antibodies against AQP8 (red) and cytochrome c (green). Colocalization of both immunoreactivities yielded a yellow merge signal. Cell nuclei were stained with 4',6-diamidine-2-phenylindol (DAPI; blue). **C**: Subcellular localization of zonula occludens-1 (ZO-1) immunoreactivity in cultured RPE cells. The arrowheads indicate staining which lines cell borders. **D**: Double immunolabeling of cell cultures with antibodies against AQP8 (red) and ZO-1 (green). **E**: Double immunolabeling of AQP8 (red) and ZO-1 (green) in an RPE monolayer freshly isolated from a donor eye. **F**: Double immunolabeling of AQP8 (red) and cytochrome c (green) in the freshly isolated RPE monolayer. Scale bars, 20 µm (**B–D**) and 10 µm (**E, F**).

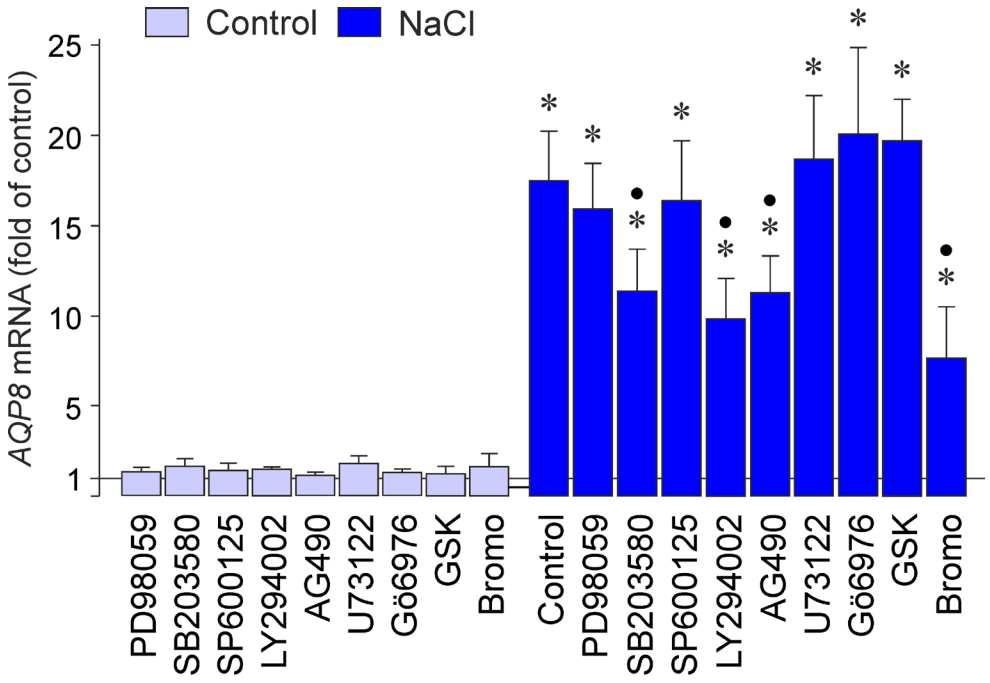

Figure 3. Intracellular signaling involved in mediating NaCl-induced expression of the *AQP8* gene in RPE cells. The level of *AQP8* mRNA was determined with real-time RT–PCR analysis in cells cultured for 6 h in iso- (control) and hyperosmotic (+ 100 mM NaCl) media (as indicated by the panels of the bars), and is expressed as folds of unstimulated control. The following agents were tested: the inhibitor of ERK1/2 activation, PD98059 (20 µM), the inhibitor of p38 MAPK activation, SB203580 (10 µM), the JNK inhibitor SP600125 (10 µM), the inhibitor of PI3K-related kinases, LY294002 (5 µM), the JAK2 inhibitor AG490 (10 µM), the PLCγ inhibitor U73122 (4 µM), the inhibitor of PKCα/β, Gö6976 (1 µM), the SGK inhibitor GSK650394 (GSK; 1 µM), and the PLA_2 inhibitor 4-bromophenacyl bromide (Bromo; 300 µM). Each bar represents mean ± standard error of the mean (SEM) obtained in three to 16 independent experiments using cell lines from different donors. Significant difference vs. unstimulated control: *p<0.05. Significant difference vs. NaCl control: •p<0.05.

no statistically significant (p>0.05) effects on *AQP8* gene expression within 6 h of stimulation with high NaCl (data not shown): the protein kinase A inhibitor H-89 (1 µM), the inhibitor of Src tyrosine kinases, PP2 (100 nM), the cyclo-oxygenase inhibitors indomethacin (10 µM), acetylsalicylic acid (2 mM), and ibuprofen (400 µM), the cyclooxygenase-2 inhibitor NS-398 (50 µM), triamcinolone acetonide (50 µM), the caspase-1 inhibitor Ac-YVAD-CMK (500 nM), the phospholipase D_1 inhibitor VU0359595 (150 nM), and the phospholipase D_2 inhibitor VU0285655–1 (500 nM). The data indicate that activation of p38 MAPK, PI3K, and JAK2 signal transduction pathways, as well as of PLA_2, is involved in mediating the full expression of the *AQP8* gene in RPE cells under high NaCl conditions.

It is unlikely that oxidative stress, e.g., induced by mitochondrial dysfunction or impaired AQP8-mediated H_2O_2 transport or both, plays a role in mediating NaCl-induced expression of the *AQP8* gene in RPE cells, because the cell-permeable reducing agent dithiothreitol (300 µM), the inhibitor of reactive oxygen species, N-acetyl-L-cysteine (1 mM), and the inhibitor of the mitochondrial permeability transition pore, cyclosporin A (1 µM [38]), had no effects on *AQP8* gene expression within 6 h of stimulation with high NaCl (data not shown). It is also unlikely that intracellular calcium signaling plays a significant role because the cell-permeable calcium chelator BAPTA/AM (5 µM), the phospholipase Cγ (PLCγ) inhibitor U73122 (Figure 3), the inhibitor of calcium-binding proteins, ruthenium red (30 µM), the inhibitor of protein kinase C (PKC) α/β, Gö6976 (Figure 3), and the calpain inhibitor, PD150606 (100 µM), had no effects on *AQP8* gene expression within 6 h of stimulation with high NaCl (data not shown).

Transcription factor activity involved in mediating NaCl-induced AQP8 gene expression: Extracellular hyperosmolarity was shown to induce the expression and activation of various transcription factors in RPE cells, including HIF-1α, nuclear factor (NF)-κB, activator protein-1 (AP-1), and NFAT5 [10,39,40]. Pharmacological blockers were used to investigate which transcription factors mediate NaCl-induced expression of the *AQP8* gene in RPE cells. As shown in Figure 4A, *AQP8* gene expression under unstimulated control conditions was statistically significantly (p<0.05) increased in the presence of the AP-1 inhibitor SR11302, suggesting that AP-1 activity exerts an inhibitory effect on constitutive expression of the *AQP8* gene in RPE cells. NaCl-induced *AQP8* gene expression was not altered in the presence of inhibitors of HIF-1 [41], signal transducer and activator of transcription 3 (STAT3) [42], NF-κB [43], and AP-1 (Figure

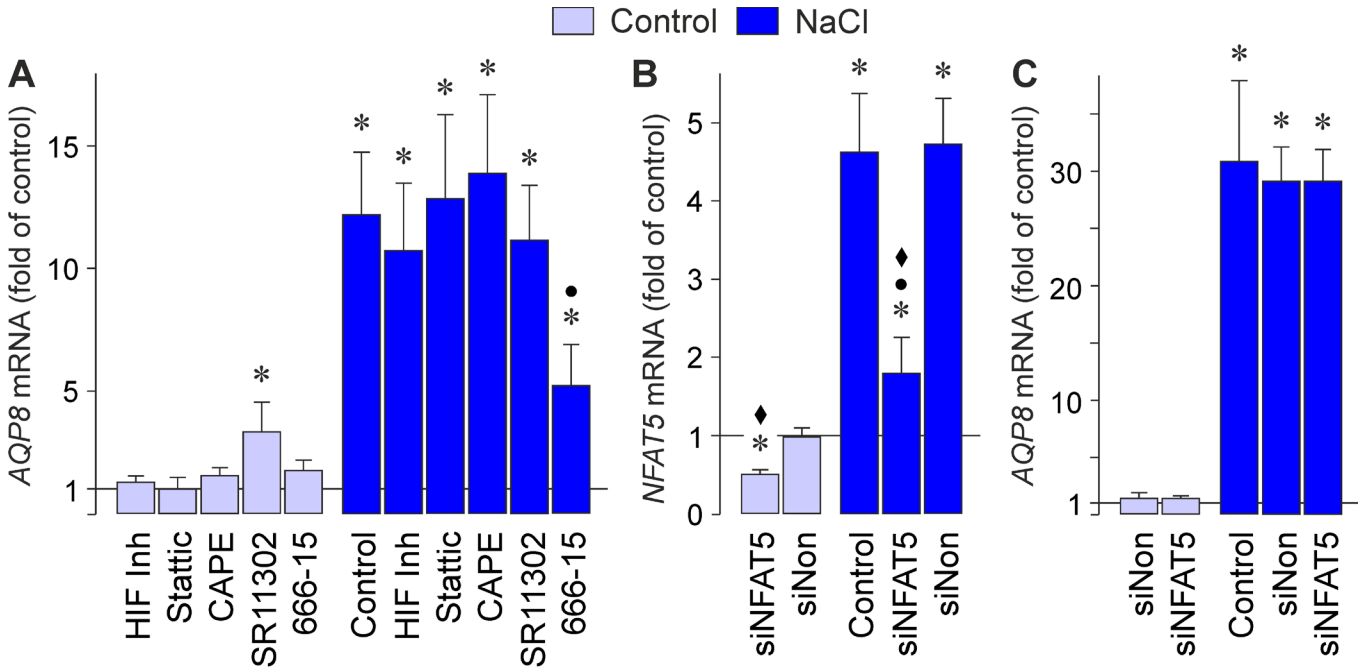

Figure 4. Transcription factor activity involved in mediating NaCl-induced expression of the *AQP8* gene in RPE cells. The mRNA levels were determined with real-time RT–PCR analysis in cells cultured for 6 h in iso- (control) and hyperosmotic (+ 100 mM NaCl) media (as indicated by the panels of the bars), and are expressed as folds of unstimulated control. **A**: The following agents were tested: an HIF-1 inhibitor (HIF-Inh; 5 µM), the STAT3 inhibitor Stattic (1 µM), the NF-κB inhibitor CAPE (5 µM), the AP-1 inhibitor SR11302 (5 µM), and the CREB inhibitor 666–15 (250 nM). **B**, **C**: Effects of knockdown of *NFAT5* gene expression with siRNA (siNFAT5; 5 nM) on *NFAT5* (**B**) and *AQP8* mRNA levels (**C**) in cells cultured for 6 h in iso- or hyperosmotic media compared to non-transfected cells (control). As negative control, nontargeted siRNA (siNon; 5 nM) was used. siRNA transfection was performed 50 h before the addition of 100 mM NaCl. Each bar represents mean ± standard error of the mean (SEM) obtained in three to 16 independent experiments using cell lines from different donors. Significant difference vs. unstimulated control: *p<0.05. Significant difference vs. NaCl control: •p<0.05. Significant difference vs. nontargeted siRNA: ♦p<0.05.

4A). However, the cAMP response element-binding protein (CREB) inhibitor 666–15 induced a statistically significant (p<0.05) decrease in NaCl-induced *AQP8* gene expression in the RPE cells (Figure 4A).

In various cell systems, cellular survival under hyperosmotic conditions depends on the transcriptional activity of NFAT5 [44]. It was shown that high extracellular NaCl induces expression of the *NFAT5* (Gene ID: 10725; OMIM: 604708) gene and NFAT5 protein, and DNA binding of NFAT5, in RPE cells [10]. To investigate whether NFAT5 activity is involved in mediating NaCl-induced expression of the *AQP8* gene in RPE cells, *NFAT5* was knocked down by transfection of the cells with NFAT5 siRNA. In accordance with a previous study [10], transfection of NFAT5 siRNA reduced the level of *NFAT5* transcripts by 50–60% in cells cultured under control and high-NaCl conditions; transfection with nontargeted siRNA had no effect (Figure 4B). However, transfection with NFAT5 siRNA or scrambled siRNA did not alter the cellular level of *AQP8* mRNA under both conditions (Figure 4C). The data suggest that NaCl-induced expression of the *AQP8* gene in RPE cells is (in part) mediated by the activity of CREB. However, it cannot be ruled out that the activities of additional transcription factors not investigated in the present study may contribute to NaCl-induced activation of the *AQP8* gene.

Receptor-mediated regulation of NaCl-induced AQP8 gene expression: Extracellular hyperosmolarity was shown to induce secretion of various growth and inflammatory factors from RPE cells, e.g., VEGF, basic fibroblast growth factor (bFGF), TGF-β1, and IL-1β [10,45]. To investigate whether autocrine/paracrine receptor signaling is required for NaCl-induced *AQP8* gene expression in RPE cells, we tested pharmacological blockers of different receptor subtypes in cultures that were stimulated for 6 h with high (+ 100 mM) NaCl. As shown in Figure 5A, the following receptor blockers had no effects on control and NaCl-induced *AQP8* gene expression: the inhibitor of the FGF receptor kinase, PD173074, the blocker of the VEGF receptor-2, SU1498, the

inhibitor of the PDGF receptor tyrosine kinase, AG1296, the blocker of the epidermal growth factor (EGF) receptor tyrosine kinase, AG1478, the inhibitor of TGF-β1 superfamily activin receptor-like kinase receptors, SB431542, and the inhibitor of various G protein-coupled receptor subtypes, suramin. In addition, the broad-spectrum matrix metalloproteinase inhibitor 1,10-phenanthroline had no effect (Figure 5A); this suggests that shedding of growth factors from the extracellular matrix is not involved in mediating expression of the *AQP8* gene. NaCl-induced expression of the *AQP8* gene in RPE cells was also not dependent on the autocrine/paracrine signaling of purinergic receptors, because suramin also inhibits several subtypes of adenosine and purinergic metabotropic (P2Y) receptors [46], and because the following antagonists of purinergic receptors had no statistically significant ($p>0.05$) effects on *AQP8* gene expression within 6 h of stimulation with high NaCl (data not shown): the $P2Y_1$ receptor antagonist MRS2179 (30 µM), the $P2Y_2$ receptor antagonist AR-C 118925XX (10 µM), the antagonist of ionotropic $P2X_7$ receptors, A-438079 (50 nM), the adenosine A_1 receptor antagonist DPCPX (50 nM), and the adenosine A_{2A} receptor antagonist CSC (200 nM). However, a recombinant IL-1 receptor antagonist increased statistically significantly ($p<0.05$) NaCl-induced *AQP8* gene expression (Figure 5A), suggesting that autocrine/paracrine IL-1 receptor signaling suppressed NaCl-induced expression of the *AQP8* gene in RPE cells. To confirm the assumption that IL-1β-mediated signaling has an inhibitory effect on *AQP8* gene expression, we tested exogenous IL-1β. As shown in Figure 5B, administration of IL-1β induced a statistically significant ($p<0.05$) decrease in NaCl-induced, but not of control, expression of the *AQP8* gene. The effect of IL-1 β was apparently not dependent on inflammasome activation because the inhibitor of the nucleotide-binding oligomerization domain receptors-like receptor protein 3 (NLRP3) inflammasome, MCC950 [47], had no effect on NaCl-induced *AQP8* gene expression,

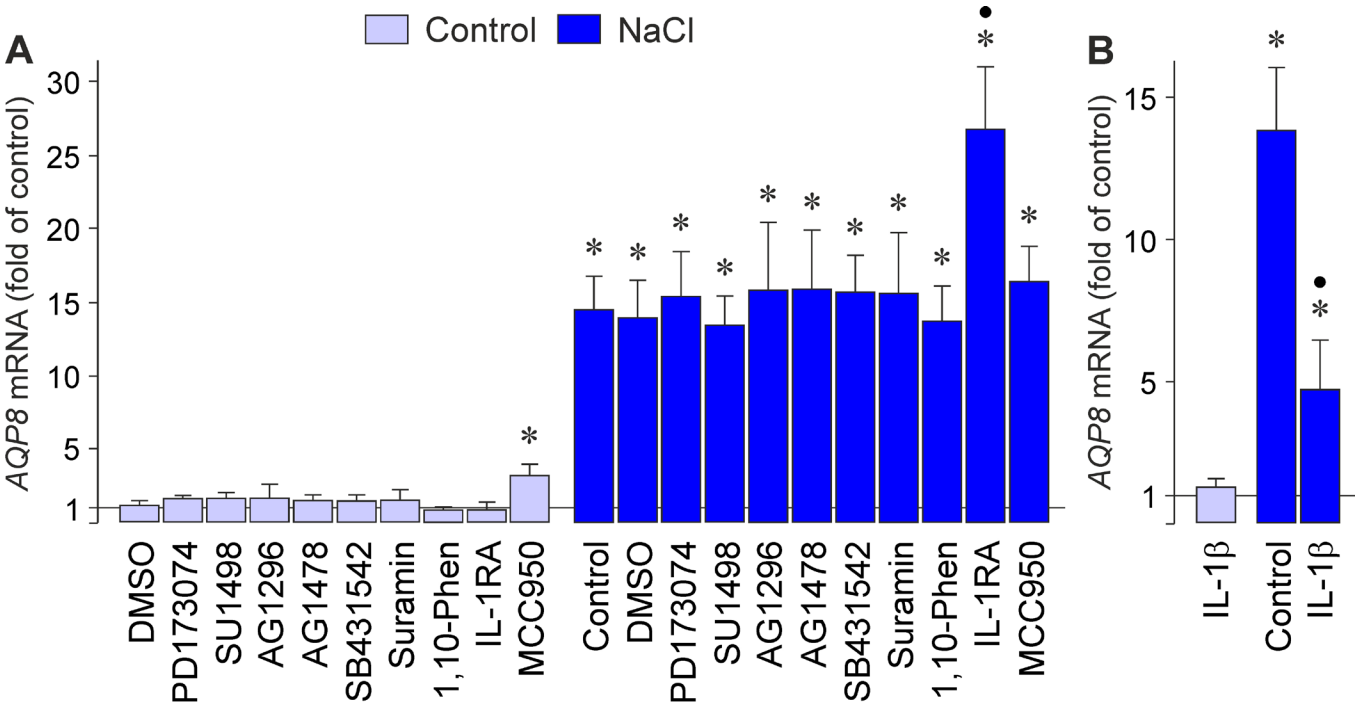

Figure 5. Receptor-mediated regulation of NaCl-induced expression of the *AQP8* gene in RPE cells. The level of *AQP8* mRNA was determined with real-time RT–PCR analysis in cells cultured for 6 h in iso- (control) and hyperosmotic (+ 100 mM NaCl) media (as indicated by the panels of the bars), and is expressed as folds of the unstimulated control. **A**: The following agents were tested: the inhibitor of the FGF receptor kinase, PD173074 (500 nM), the blocker of VEGF receptor-2, SU1498 (10 µM), the inhibitor of the PDGF receptor tyrosine kinase, AG1296 (10 µM), the blocker of the EGF receptor tyrosine kinase, AG1478 (600 nM), the inhibitor of TGF-β1 superfamily activin receptor-like kinase receptors, SB431542 (10 µM), the inhibitor of various G protein-coupled receptor subtypes, suramin (200 µM), the broad-spectrum matrix metalloproteinase inhibitor 1,10-phenanthroline (1,10-Phen; 10 µM), a recombinant human IL-1 receptor antagonist (IL-1RA; 1 µg/ml), and the NLRP3 inflammasome inhibitor MCC950 (1 µM). **B**: Effect of exogenous IL-1β (10 ng/ml) on *AQP8* gene expression. Vehicle control was made with dimethyl sulfoxide (DMSO; 1:500). Each bar represents mean ± standard error of the mean (SEM) obtained in three to ten independent experiments using cell lines from different donors. Significant difference vs. unstimulated control: *$p<0.05$. Significant difference vs. NaCl control: •$p<0.05$.

while the inhibitor increased the expression under control conditions (Figure 5A).

Plasma membrane channels involved in mediating NaCl-induced AQP8 gene expression: In addition to AQP-mediated water flux, channel-mediated ion currents contribute to the compensation of osmotic gradients across the plasma membrane under aniso-osmotic conditions [48]. One subtype of potassium channels, K_{ATP} channels, which are heteromultimers of pore-forming Kir6.x subunits and the regulatory subunit sulfonylurea receptor (SUR) [49], was found to be expressed in RPE cells [50,51]. We tested two sulfonylureas, glibenclamide and glipizide, which induce, after binding to SUR, the closure of K_{ATP} channels and of ATP-sensitive nonselective cation channels $NC_{Ca\text{-}ATP}$ [52,53]. As shown in Figure 6A, glibenclamide and glipizide caused statistically significant ($p<0.05$) decreases of NaCl-induced *AQP8* gene expression in RPE cells. However, the competitive blocker of organic anion transporters, probenecid [54], had no effect (Figure 6A). Glibenclamide was also shown to inhibit activation of the NLRP3 inflammasome [55]. However, because the NLRP3 inflammasome inhibitor MCC950 had no effect on NaCl-induced *AQP8* gene expression (Figure 5A), it is unlikely that the effects of sulfonylureas on *AQP8* gene expression are mediated by inhibition of the NLRP3 inflammasome. To further investigate whether the activity of K_{ATP} channels influences expression of the *AQP8* gene, we tested the channel opener pinacidil, which is an activator of SUR2A and SUR2B, but not SUR1 [56]. As shown in Figure 6B, pinacidil induced an increase in the expression level of the *AQP8* gene after 24 h of stimulation. This suggests that activation of K_{ATP} channels stimulates *AQP8* gene expression.

In addition to sulfonylureas, carbenoxolone decreased NaCl-induced *AQP8* gene expression in RPE cells statistically significantly ($p<0.05$; Figure 6A). Carbenoxolone is an inhibitor of the steroid 11β-hydroxylase and of pannexin hemichannels [57,58]. There are two steroid 11β-hydroxylase isozymes encoded by the *CYP11B1* (Gene ID: 1584; OMIM: 610613) and *CYP11B2* (Gene ID: 1585; OMIM: 124080)

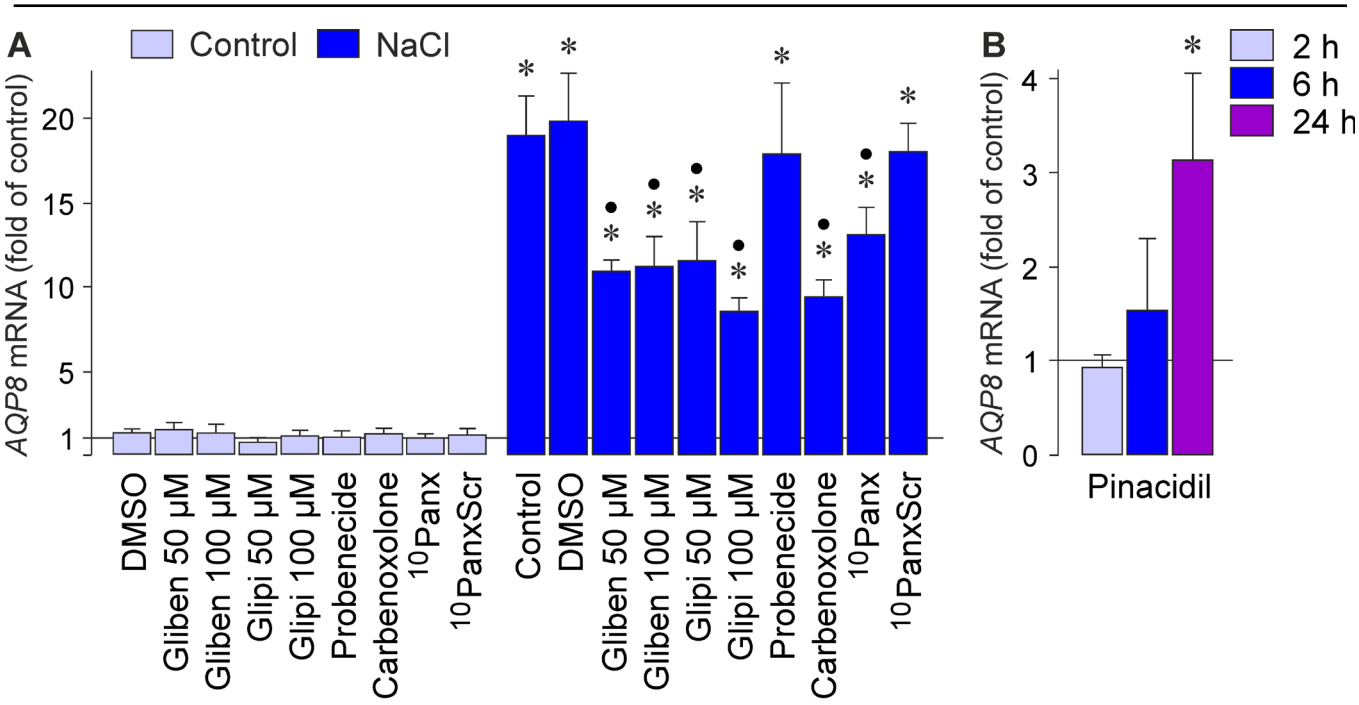

Figure 6. Plasma membrane channel-mediated regulation of NaCl-induced expression of the *AQP8* gene in RPE cells. **A**: The level of *AQP8* mRNA was determined with real-time RT–PCR analysis in cells cultured for 6 h in iso- (control) and hyperosmotic (+ 100 mM NaCl) media (as indicated by the panels of the bars), and is expressed as folds of unstimulated control. The following agents were tested: the sulfonylureas glibenclamide (Gliben; 50 and 100 µM) and glipizide (Glipi; 50 and 100 µM), the blocker of organic anion transporters, probenecide (1 mM), the pannexin inhibitor carbenoxolone (5 µM), the pannexin-blocking peptide ^{10}panx (200 µM), and the scrambled control peptide ^{10}panxScr (200 µM). Vehicle control was made with dimethyl sulfoxide (DMSO; 1:500). **B**: Effect of pinacidil (100 µM) on expression of the *AQP8* gene under control conditions. The mRNA level was determined in cells cultured for 2, 6, and 24 h (as indicated by the panels of the bars), and is expressed as folds of unstimulated control. Each bar represents mean ± standard error of the mean (SEM) obtained in three to ten independent experiments using cell lines from different donors. Significant difference vs. unstimulated control: *$p<0.05$. Significant difference vs. NaCl control: •$p<0.05$.

genes; however, transcripts of both genes were not detected in the RNA extracted from the cells used (data not shown). Therefore, the effect of carbenoxolone was likely mediated by blocking pannexins. To prove this assumption, we tested the pannexin-blocking peptide ^{10}panx. As shown in Figure 6A, the peptide decreased statistically significantly ($p<0.05$) NaCl-induced *AQP8* gene expression in RPE cells, whereas a scrambled control peptide had no effect (Figure 6A).

Expression of K_{ATP} channel subunits: The data suggest that activation of K_{ATP} channels is involved in mediating hyperosmotic expression of the *AQP8* gene in RPE cells. Coexpression of the K_{ATP} channel subunits Kir6.2 and SUR1 was described in the rat RPE [50]. We investigated whether human RPE cells express K_{ATP} channel subunits. As shown in Figure 7A,B, acutely isolated and cultured human RPE cells contained *Kir6.1* but not *Kir6.2* transcripts. The expression level of the *Kir6.1* gene was not different between acutely isolated and cultured cells (Figure 7B). Cultured cells also contained *SUR2B* (Gene ID: 10060; OMIM: 601439), but not *SUR1* (Gene ID: 6833; OMIM: 600509) and *SUR2A* (Gene ID: 10060; OMIM: 601439), transcripts (Figure 7A). The expression levels of the *Kir6.1* and *SUR2B* genes were not altered under hyperosmotic compared to control conditions (Figure 7C). Cultured RPE cells were labeled with an antibody against Kir6.1 (Figure 7D).

Effects of AQP8 knockdown on RPE cell proliferation and viability: To investigate whether AQP8 modulates the proliferation and viability of RPE cells, we knocked down *AQP8* with siRNA. As shown in Figure 8A, transfection with AQP8 siRNA reduced the level of *AQP8* transcripts by 60–75% in cells cultured under control conditions; transfection with scrambled nontargeted siRNA had no effect. Transfection with AQP8 siRNA also reduced statistically significantly ($p<0.05$) the level of *AQP8* mRNA in cells cultured under high NaCl conditions and in the presence of $CoCl_2$, respectively, when compared to the respective controls and the effects of nontargeted siRNA (Figure 8B).

It was described that high extracellular osmolarity induces cell cycle arrest in various cell systems, including RPE cells [59,60]. High extracellular NaCl and the addition of the hypoxia mimetic $CoCl_2$ to the culture medium induced decreases in the RPE cell proliferation rate (data not shown), as previously described [61]. Transfection of AQP8 siRNA had no effects on the proliferation rate under control, high (+100 mM) NaCl, and $CoCl_2$ (150 µM)-stimulated conditions (data not shown), suggesting that the activity of AQP8 does not influence the proliferation of RPE cells.

It was shown in various cell types that AQP8-mediated water and H_2O_2 transport contributes to the regulation of cell survival under stress conditions [62]. In the cultured RPE cells, high extracellular NaCl caused a slight increase in cell viability, while cell culture in a $CoCl_2$-containing medium was associated with a decrease in viability (Figure 8C). Cells transfected with AQP8 siRNA displayed statistically significantly ($p<0.05$) lower viability than non-transfected cells and cells transfected with nontargeted siRNA; this was found under all conditions tested (Figure 8C).

Effect of AQP8 knockdown on the expression and secretion of VEGF: VEGF is a factor secreted by RPE cells implicated in the pathogenesis of different blinding retinal diseases, such as retinal edema and neovascular AMD [63]. To investigate whether AQP8 modulates the expression and secretion of VEGF from RPE cells, we knocked down *AQP8* with siRNA. Transfection of RPE cells with AQP8 siRNA had no statistically significant ($p>0.05$) effects on the cellular level of the *VEGFA* mRNA under unstimulated control and high NaCl conditions (Figure 9A). However, in $CoCl_2$-induced chemical hypoxia, cells that were transfected with AQP8 siRNA displayed a statistically significantly ($p<0.05$) higher expression level of *VEGFA* mRNA compared to non-transfected cells and cells that had been transfected with nontargeted siRNA (Figure 9A). NaCl-induced extracellular hyperosmolarity and hypoxia caused the secretion of VEGF from the RPE cells, as indicated by the elevated levels of the VEGF-A protein in the cultured media compared to the non-stimulated control (Figure 9B). Transfection of AQP8 siRNA did not statistically significantly ($p>0.05$) alter the VEGF-A content of the cultured media under unstimulated control conditions and in the presence of high NaCl (Figure 9B). However, when the cells were cultured in the presence of $CoCl_2$ or in a 0.2% O_2 atmosphere, the media of the cells transfected with AQP8 siRNA contained statistically significantly higher ($p<0.05$) levels of VEGF-A protein compared to the media of non-transfected cells and of cells that had been transfected with nontargeted siRNA (Figure 9B). The data show that the knockdown of *AQP8* results in stimulation of hypoxic expression and secretion of VEGF from RPE cells.

DISCUSSION

One major function of the RPE is the transport of excess subretinal water and potassium into the choroidal blood [6]. In many cell types, bidirectional transport of water across membranes is facilitated by AQP water channels [7]. In addition to transcripts of other AQP subtypes, human RPE cells contain *AQP8* gene transcripts [8,10]. In the present study, we investigated the subcellular expression of AQP8 and the cellular mechanisms of hyperosmotic *AQP8* gene expression in cultured human RPE cells. We found that expression of

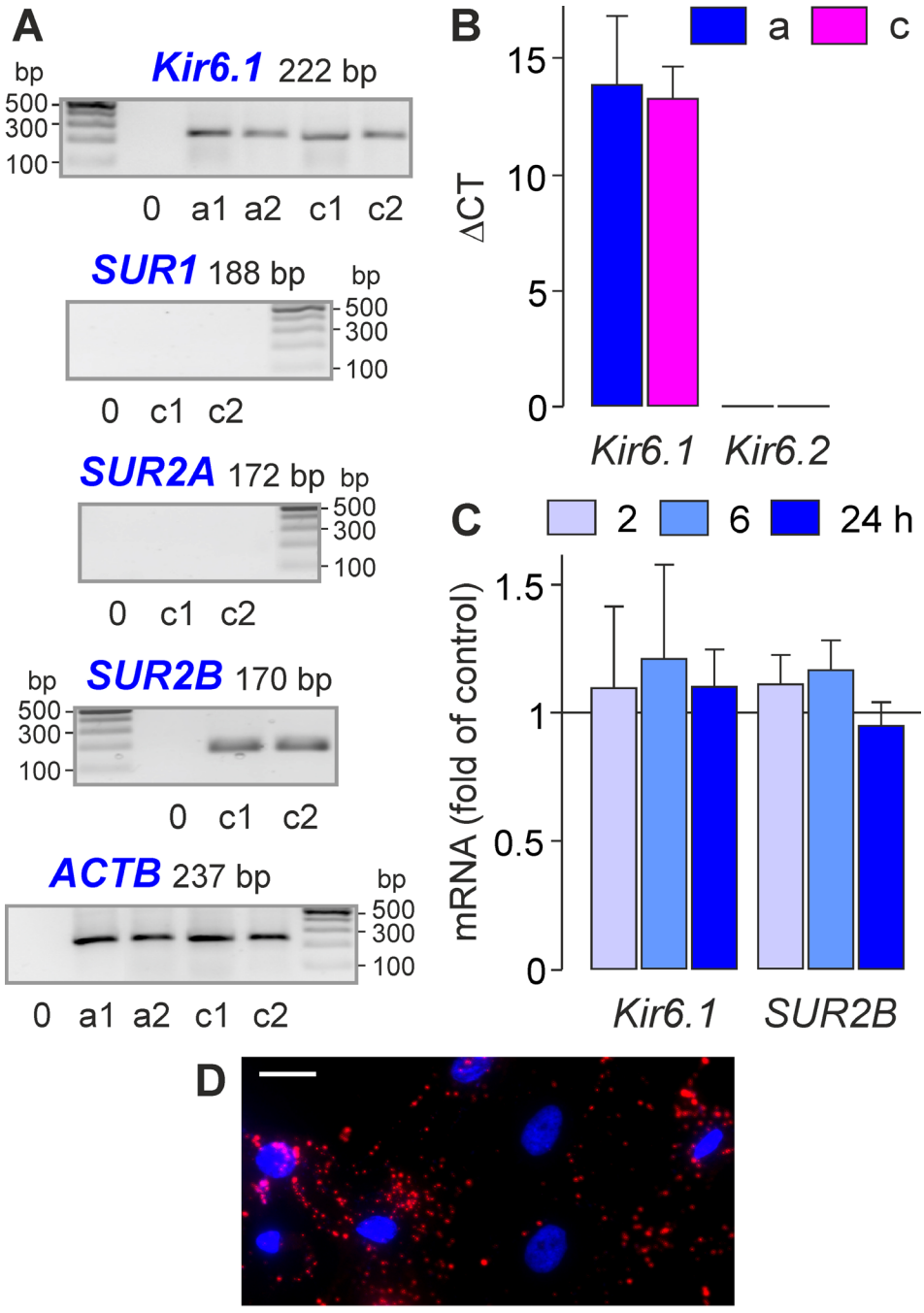

Figure 7. Expression of K_{ATP} channel subunits in human RPE cells. **A**: Presence of *Kir6.1* and *SUR2B* gene transcripts in acutely isolated (a) and cultured (c) human RPE cells, as determined with RT–PCR analysis. The correct lengths of the PCR products were confirmed with agarose gel electrophoresis using products obtained from cell lines of four different donors. Negative controls (0) were performed with double-distilled water instead of cDNA as the template. *ACTB* mRNA was used as loading control. **B**: Relative levels of *Kir6.1* and *Kir6.2* transcripts in acutely isolated (a) and cultured (c) RPE cells. The levels are shown as normalized cycle thresholds (ΔCT) required to detect the mRNA in real-time RT–PCR analysis. **C**: Effect of high (+ 100 mM) NaCl on the expression levels of *Kir6.1* and *SUR2B* genes. The mRNA levels were determined with real-time RT–PCR analysis in cells cultured for 2, 6, and 24 h in the hyperosmotic medium (as indicated by the panels of the bars), and are expressed as folds of unstimulated control. **D**: Cultured RPE cells were immunolabeled with an antibody against Kir6.1 (red). Cell nuclei were stained with 4',6-diamidine-2-phenylindol (DAPI; blue). Scale bar, 20 µm. In **B** and **C**, each bar represents mean ± standard error of the mean (SEM) obtained in four to six independent experiments using cell lines from different donors. Significant difference vs. unstimulated control: *p<0.05.

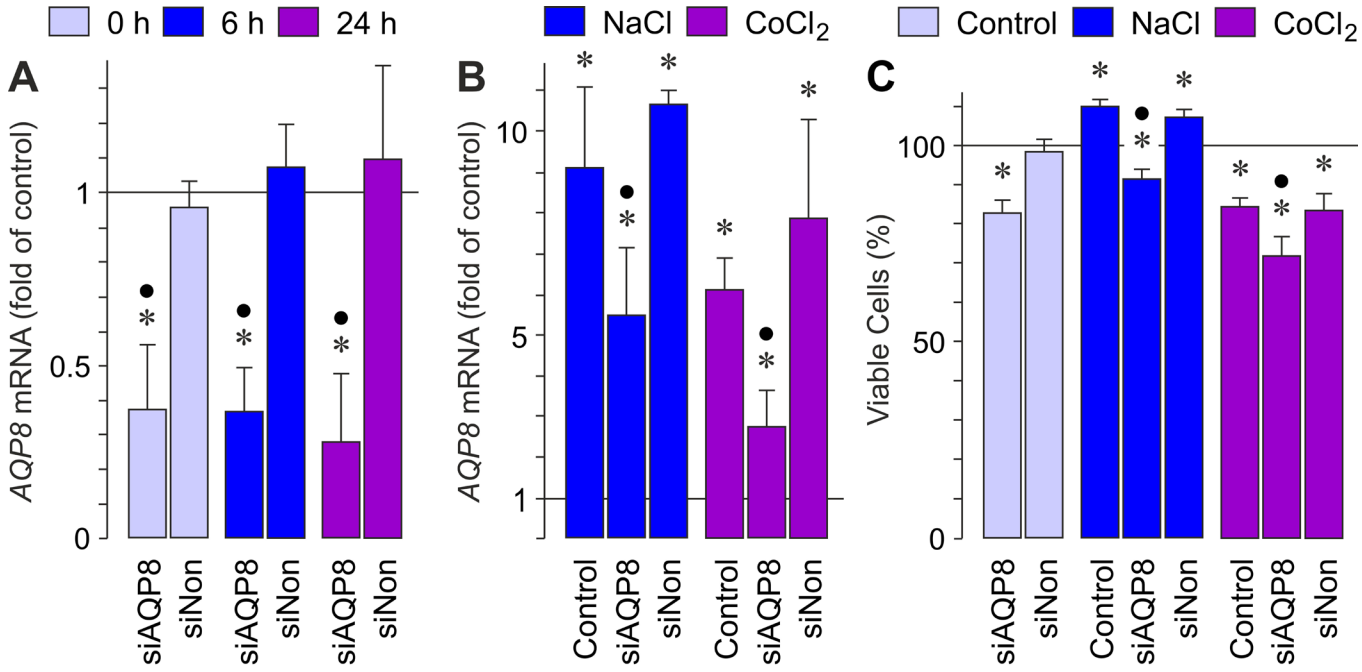

Figure 8. Effects of the knockdown of AQP8 gene expression with AQP8 siRNA (siAQP8) on the AQP8 mRNA level and the viability of cultured RPE cells. As negative control, scrambled nontargeted siRNA (siNon; 10 nM) was used. siRNA transfection was performed 24 h before the addition of 100 mM NaCl or $CoCl_2$ (150 µM). In **A** and **B**, the mRNA level is shown as folds of unstimulated control. **A**: Effects of siAQP8 and siNon on the level of *AQP8* mRNA in cells cultured for 0, 6, and 24 h under unstimulated control conditions in serum-free medium. siRNA transfection was performed 24 h before. **B**: Effects of siAQP8 (10 nM) and siNon on the level of *AQP8* mRNA in cells cultured for 6 h in a high-NaCl medium and for 24 h in the presence of $CoCl_2$, respectively. **C**: Viability of RPE cells. The data were obtained in cells cultured for 24 h in iso- (control) and hyperosmotic (high NaCl) media, and in the presence of $CoCl_2$, respectively, and are expressed as percent of unstimulated control (100%). Each bar represents mean ± standard error of the mean (SEM) obtained in five to eight independent experiments using cell lines from different donors. Significant difference vs. unstimulated control: *p<0.05. Significant difference vs. siNon and vs. NaCl and $CoCl_2$ controls, respectively: ●p<0.05.

the *AQP8* gene in RPE cells is dependent on extracellular osmolarity; it is transiently increased under hyperosmotic conditions (Figure 1B) and shows biphasic regulation under hypo-osmotic conditions (Figure 1D). *AQP8* gene expression is also increased under hypoxic and oxidative stress conditions (Figure 1E), and in the presence of the anti-inflammatory glucocorticoid triamcinolone acetonide (Figure 1F). Western blotting and immunocytochemical data suggest that the AQP8 protein is mainly located in mitochondria (Figure 2A,B,F). However, because we found different bands of AQP8 immunoreactivity in western blots of RPE cell lysates (Figure 2A), it cannot be ruled out that a minor portion of AQP8 is also present in the plasma membrane.

We found that coaddition of NaCl and sucrose did not cause an additive increase in *AQP8* gene expression after 2 h of stimulation (Figure 1B). The absence of an additive effect might be explained by the assumption that extracellular hyperosmolarity, but not the alteration of the transmembrane NaCl gradient, triggered expression of the *AQP8* gene at this time point. The statistically significant difference (p<0.05) between the *AQP8* expression levels induced by high NaCl and sucrose after 6 h of stimulation (Figure 1B) might be explained by the assumption that, at this time point, extracellular hyperosmolarity and the alteration in the transmembrane NaCl gradient induced *AQP8* gene expression.

We found that activation of the p38 MAPK and PI3K signal transduction pathways contributes to the full NaCl-induced expression of the *AQP8* gene (Figure 3). Interestingly, it was described that AQP8 is capable of increasing H_2O_2-induced phosphorylation of p38 MAPK and PI3K [27]. We also found that inhibition of PLA_2 decreases osmotic expression of the *AQP8* gene in RPE cells (Figure 3). Osmotic challenge is a known activator of PLA_2 [64]. Activation of PLA_2 is a critical factor that mediates *AQP3* [8] and *AQP8* gene expression in RPE cells (Figure 3). However, *AQP3* gene expression was shown to be induced by arachidonic acid and prostaglandin E_2 [8], while AQP8 gene expression is not (data not shown). We also found that autocrine/paracrine IL-1

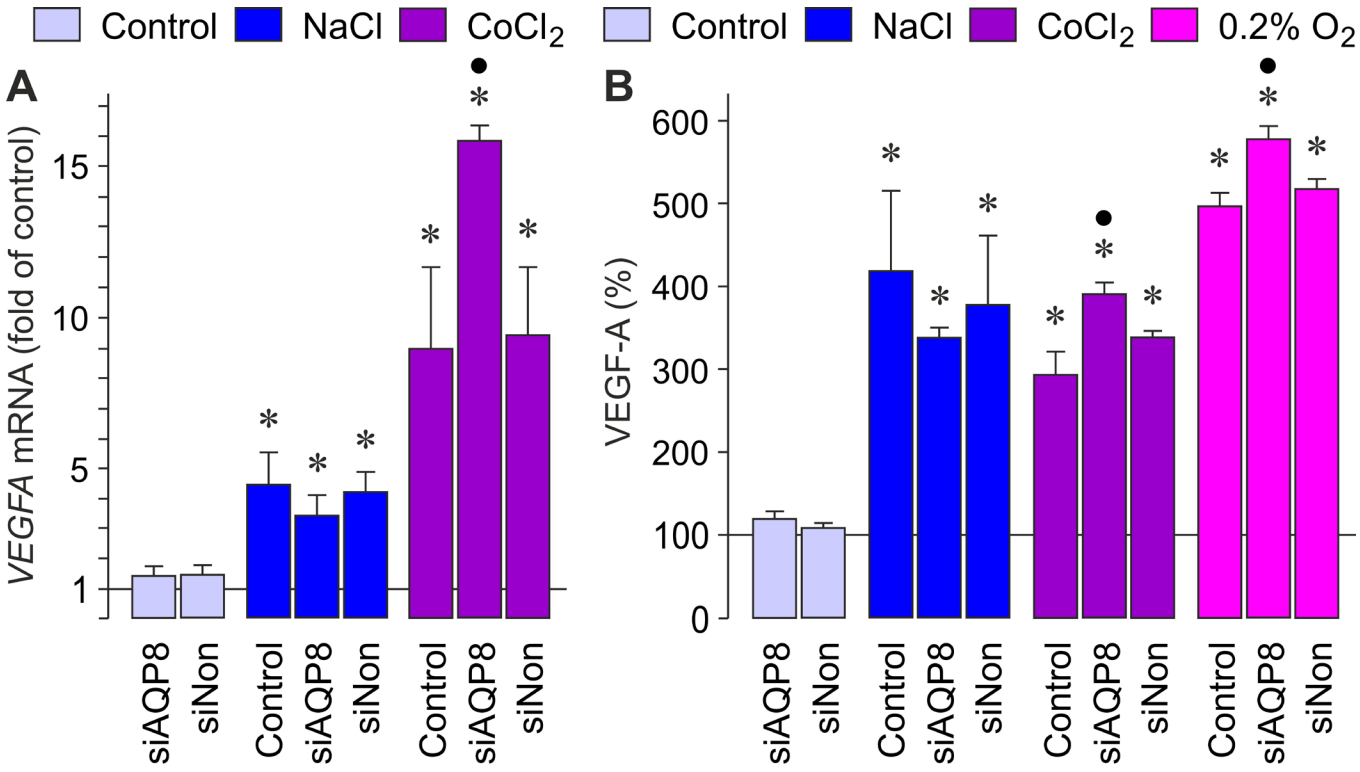

Figure 9. Effects of the knockdown of *AQP8* gene expression with siRNA (siAQP8; 10 nM) on the expression and secretion of VEGF from cultured RPE cells. As negative control, scrambled nontargeted siRNA (siNon; 10 nM) was used. siRNA transfection was performed 24 h before the addition of 100 mM NaCl or $CoCl_2$ (150 µM), and the culture in a 0.2% O_2 atmosphere, respectively. **A**: Effects of siAQP8 and siNon on the level of *VEGFA* mRNA in cells cultured for 6 h in a high-NaCl medium and in the presence of $CoCl_2$, respectively. The mRNA level is shown as folds of unstimulated control. **B**: Effects of siAQP8 and siNon on the secretion of VEGF. The level of the VEGF-A protein was determined with enzyme-linked immunosorbent assay (ELISA) in the media of cells cultured for 24 h in the presence of high NaCl and $CoCl_2$, and in a 0.2% O_2 atmosphere, respectively. The protein level is expressed as percent of unstimulated control (100%). Each bar represents mean ± standard error of the mean (SEM) obtained in four to nine independent experiments using cell lines from different donors. Significant difference vs. unstimulated control: *p<0.05. Significant difference vs. siNon and vs. NaCl, $CoCl_2$, and low-O_2 controls, respectively: ●p<0.05.

receptor signaling induced by high NaCl depresses hyperosmotic expression of the *AQP8* gene in RPE cells (Figure 5A, B). Most of the blocking agents used in the present study did not inhibit completely hyperosmotic induction of the *AQP8* gene. This may suggest that multiple signal transduction pathways contribute to osmotic induction of the *AQP8* gene.

The high NaCl-induced expression of the *AQP8* gene in RPE cells was decreased by the sulfonylureas glibenclamide and glipizide (Figure 6A). This suggests that activation of K_{ATP} and $NC_{Ca\text{-}ATP}$ channels plays a role in mediating the effect of high NaCl on expression of the *AQP8* gene. The K_{ATP} channel opener pinacidil induced a time-dependent increase in the expression level of the *AQP8* gene (Figure 6B). This could be explained by the fact that increased transmembrane ion currents must be, for osmotic reasons, accompanied by facilitated water transport. We found expression of *Kir6.1* and *SUR2B* in human RPE cells (Figure 7A,B,D). However, it cannot be ruled out that additional subtypes of potassium channels that are associated with SUR2B may contribute to the effects of the sulfonylureas on NaCl-induced expression of the *AQP8* gene. The incomplete action of the K_{ATP} channel blockers (Figure 6A) might be explained by the assumption that currents through other subtypes of potassium channels compensate, in part, the blocked currents through K_{ATP} channels, or that AQP8-mediated water transport also supports the potassium currents through other subtypes of potassium channels, or both.

K_{ATP} and $NC_{Ca\text{-}ATP}$ channels are activated by depletion of intracellular ATP [65]. Closure of the K_{ATP} channels results in a reduction in the potassium efflux from the cells, membrane depolarization, and activation of voltage-gated calcium channels [66]. In reactive astrocytes, opening of $NC_{Ca\text{-}ATP}$ channels

causes complete plasma membrane depolarization and cell blebbing; both are characteristics of cytotoxic edema [65]. Cell depolarization and blebbing induced by depletion of intracellular ATP are prevented by glibenclamide, consistent with a role for $NC_{Ca\text{-}ATP}$ channels in mediating cytotoxic edema [65]. K_{ATP} channels are known to play an important role in the ischemic preconditioning of the retina [50]. Generally, mitochondria and their K_{ATP} channels are crucially involved in mediating ischemic preconditioning in different tissues [67,68]. However, it is unlikely that mitochondrial dysfunction is involved in mediating NaCl-induced expression of the *AQP8* gene in RPE cells because the inhibitor of mitochondrial permeability transition, cyclosporin A, had no effect (data not shown). In addition, AQP8-mediated H_2O_2 transport seems to be less relevant for high NaCl-induced induction of the *AQP8* gene in RPE cells, because reducing agents and inhibitors of reactive oxygen species had no effects (data not shown). It is suggested that NaCl-induced induction of the *AQP8* gene in RPE cells facilitates transmembrane water transport which supports ion currents, e.g., potassium currents through K_{ATP} channels, that mediate the rapid compensation of the ionic and osmotic gradients across the plasma membrane under high NaCl conditions.

It was described that high extracellular NaCl induces pannexin-mediated release of ATP from RPE cells [69]. We found that inhibition of pannexins decreases NaCl-induced expression of the *AQP8* gene (Figure 6A), suggesting that activation of pannexins is required for full *AQP8* gene expression in RPE cells. However, *AQP8* gene expression was not altered in the presence of inhibitors of various subtypes of purinergic receptors (data not shown). In cultured astrocytes, activation of pannexin-1 was shown to be involved in mediating the expression of AQP4 and the release of IL-1β under conditions of experimental ischemia [70]. The functional role of pannexin activation in mediating high NaCl-induced *AQP8* gene expression in RPE cells remains to be investigated.

In different cell systems, AQP8 activity either amplifies cell proliferation, e.g., via facilitating H_2O_2-mediated tyrosine kinase signaling upon activation of growth factor receptors [27], or inhibits cell proliferation, via inactivation of PI3K-mediated signaling [71]. In glioma cells, knockdown of *AQP8* induces cell cycle arrest, via downregulation of cell cycle proteins [72]. We found that transfection of AQP8 siRNA had no effects on the proliferation rate of RPE cells (data not shown).

Different effects of *AQP8* knockdown on cell viability were described in various cell systems. In hepatoma cells, knockdown of *AQP8* causes mitochondrial depolarization and necrotic cell death which was attributed to the reduced H_2O_2 extrusion from the mitochondria resulting in an increased mitochondrial reactive oxygen species level [29]. In 3T3-L1 preadipocytes, which express AQP8 predominantly in mitochondria, knockdown of *AQP8* results in mitochondrial swelling, but has no effect on cell viability [24]. Because cellular shrinkage mediated by ion and water efflux is a crucial step in apoptotic cell death [73], knockdown of *AQP*s may increase resistance to apoptosis [74]. We found that knockdown of *AQP8* reduces RPE cell viability under control, hyperosmotic, and hypoxic conditions (Figure 8C). This result suggests that water or H_2O_2 transport or both through AQP8 is required for the full viability of RPE cells under various conditions. It was shown that mitochondrial oxidative stress in the RPE leads to localized retinal degeneration [75], and that high salt loading in rats causes intracellular edema and mitochondrial swelling in retinal ganglion and glial cells [20]. It could be that knockdown of *AQP8* impairs water and H_2O_2 transport through mitochondrial membranes which results in a decrease in the viability of RPE cells. The relatively small effects of *AQP8* knockdown on cell viability (10–20% decrease) are statistically significant and might be explained by the fact that the siRNA used caused a decrease in the *AQP8* transcript level by only 60–75% (Figure 8A, B) and with the assumption that a part of the lost AQP8-mediated transmembrane water transport may be compensated by other subtypes of aquaporins. The decrease in ATP production induced by *AQP8* knockdown may activate K_{ATP} channels. However, we found that the activity of K_{ATP} channels is implicated in mediating *AQP8* gene expression under hyperosmotic, but not under control, conditions (Figure 6A). Further research is necessary to determine the mechanisms of the involvement of AQP8 in the maintenance of RPE cell viability. Triamcinolone acetonide, an anti-inflammatory steroid clinically used for rapid resolution of retinal edema [76], induced expression of the *AQP8* gene under control conditions (Figure 1F), but not under hyperosmotic conditions (data not shown). An improvement in AQP8-mediated transmembrane transport of water and H_2O_2 by triamcinolone acetonide may contribute to the edema-resolving effect of this steroid, and may protect mitochondrial function and integrity in RPE cells.

VEGF is the most relevant hypoxia-induced angiogenic factor which promotes retinal edema and choroidal neovascularization [63]. VEGF expression and secretion are also induced by other pathogenic conditions, e.g., extracellular hyperosmolarity and H_2O_2-induced oxidative stress [10,77]. We found that knockdown of *AQP8* stimulated expression and secretion of VEGF under hypoxic conditions and had no effects under control and high NaCl conditions (Figure 9A,B). The effect of *AQP8* knockdown specifically under hypoxic

conditions might be explained by the fact that hypoxia affects the mitochondrial oxidative stress level. It was shown that administration of a mitochondria-targeted antioxidant decreases the retinal VEGF mRNA and protein levels in OXYS rats, an animal model of AMD [78]. Mitochondrial complex III senses hypoxic conditions and generates reactive oxygen species which stabilize HIF-1α protein that induces transcription of the *VEGFA* (Gene ID: 7422; OMIM: 192240) gene [79]. Inhibition of AQP8-mediated H_2O_2 transport by gene knockdown may exacerbate these conditions, resulting in increased expression of the *VEGFA* gene. VEGF is known to promote mitochondrial function and biogenesis [80,81]. It could be that mitochondrial dysfunction induced by coadministration of $CoCl_2$ and AQP8 siRNA induces expression and release of VEGF to stimulate mitochondrial function and biogenesis in an autocrine/paracrine manner.

We found statistically significant effects of high extracellular NaCl on expression of the *AQP8* gene when more than 10 mM NaCl were added to the culture medium (Figure 1C). It is generally accepted that the highest pathological blood osmolality in human subjects is around 360 mOsm/kg which can be achieved with the addition of 40 mM NaCl to the culture medium [82,83]. However, less well appreciated is that the local extracellular NaCl concentration in the interstitium may be considerably higher (160–250 mM) than the plasma concentration of NaCl (about 140 mM) [84,85]. Therefore, the present results may have relevance for in vivo conditions.

RPE cells express different AQP subtypes, including AQP1, AQP3, AQP5, and AQP8 [5,8-10]. The AQP subtypes may have different functional roles in mediating water transport through RPE cells. It is conceivable that AQP1, which is not regulated by extracellular osmolarity [10], facilitates constitutive water transport through RPE cells. AQP3 and AQP5 may facilitate osmotic water transport under partly different conditions and with partly different functions; AQP3 is upregulated under inflammatory conditions [8] and may mediate glycerol transport. AQP8 may facilitate mitochondrial water and H_2O_2 transport. Further research is required to determine the functional roles of the different AQP subtypes in RPE cells.

ACKNOWLEDGMENTS

The authors thank Ute Weinbrecht for excellent technical assistance.

REFERENCES

1. Bresnick GH. Diabetic maculopathy. A critical review highlighting diffuse macular edema. Ophthalmology 1983; 90:1301-17. [PMID: 6664669].
2. Bressler NM, Bressler SB, Fine SL. 2001. Neovascular (exudative) age-related macular degeneration. In: Schachat AP (ed) *Retina*. Mosby, St Louis, 2001, pp 1100–35.
3. Bringmann A, Reichenbach A, Wiedemann P. Pathomechanisms of cystoid macular edema. Ophthalmic Res 2004; 36:241-9. [PMID: 15583429].
4. Nagelhus EA, Horio Y, Inanobe A, Fujita A, Haug FM, Nielsen S, Kurachi Y, Ottersen OP. Immunogold evidence suggests that coupling of K^+ siphoning and water transport in rat retinal Müller cells is mediated by a coenrichment of Kir4.1 and AQP4 in specific membrane domains. Glia 1999; 26:47-54. [PMID: 10088671].
5. Stamer WD, Bok D, Hu J, Jaffe GJ, McKay BS. Aquaporin-1 channels in human retinal pigment epithelium: Role in transepithelial water movement. Invest Ophthalmol Vis Sci 2003; 44:2803-8. [PMID: 12766090].
6. Strauss O. The retinal pigment epithelium in visual function. Physiol Rev 2005; 85:845-81. [PMID: 15987797].
7. Agre P, King LS, Yasui M, Guggino WB, Ottersen OP, Fujiyoshi Y, Engel A, Nielsen S. Aquaporin water channels - from atomic structure to clinical medicine. J Physiol 2002; 542:3-16. [PMID: 12096044].
8. Hollborn M, Ulbricht E, Reichenbach A, Wiedemann P, Bringmann A, Kohen L. Transcriptional regulation of aquaporin-3 in human retinal pigment epithelial cells. Mol Biol Rep 2012; 39:7949-56. [PMID: 22535323].
9. Hollborn M, Rehak M, Iandiev I, Pannicke T, Ulbricht E, Reichenbach A, Wiedemann P, Bringmann A, Kohen L. Transcriptional regulation of aquaporins in the ischemic rat retina: Upregulation of aquaporin-9. Curr Eye Res 2012; 37:524-31. [PMID: 22577771].
10. Hollborn M, Vogler S, Reichenbach A, Wiedemann P, Bringmann A, Kohen L. Regulation of the hyperosmotic induction of aquaporin 5 and VEGF in retinal pigment epithelial cells: Involvement of NFAT5. Mol Vis 2015; 21:360-77. [PMID: 25878490].
11. Reichenbach A, Bringmann A. Retinal Glia. In: Verkhratsky A, Parpura V (eds) *Colloquium Series on Neuroglia in Biology and Medicine: From Physiology to Disease.* Morgan & Claypool Life Sciences, Philadelphia, PA, 2015, pp 313–331.
12. Neuhofer W. Role of NFAT5 in inflammatory disorders associated with osmotic stress. Curr Genomics 2010; 11:584-90. [PMID: 21629436].
13. Klein R, Klein BE, Moss SE, Cruickshanks KJ. The Wisconsin Epidemiologic Study of Diabetic Retinopathy: XVII. The 14-year incidence and progression of diabetic retinopathy and associated risk factors in type 1 diabetes. Ophthalmology 1998; 105:1801-15. [PMID: 9787347].
14. Kamoi K, Takeda K, Hashimoto K, Tanaka R, Okuyama S. Identifying risk factors for clinically significant diabetic

macula edema in patients with type 2 diabetes mellitus. Curr Diabetes Rev 2013; 9:209-17. [PMID: 23363297].

15. Hammes HP. Pathophysiological mechanisms of diabetic angiopathy. J Diabetes Complications 2003; 17:Suppl16-9. [PMID: 12623164].

16. Klein R, Klein BE, Tomany SC, Cruickshanks KJ. The association of cardiovascular disease with the long-term incidence of age-related maculopathy: the Beaver Dam Eye Study. Ophthalmology 2003; 110:1273-80. [PMID: 12799274].

17. Van Leeuwen R, Ikram MK, Vingerling JR, Witteman JC, Hofman A, de Jong PT. Blood pressure, atherosclerosis, and the incidence of age-related maculopathy: the Rotterdam Study. Invest Ophthalmol Vis Sci 2003; 44:3771-7. [PMID: 12939290].

18. Lifton RP, Gharavi AG, Geller DS. Molecular mechanisms of human hypertension. Cell 2001; 104:545-56. [PMID: 11239411].

19. Iandiev I, Pannicke T, Reichenbach A, Wiedemann P, Bringmann A. Diabetes alters the localization of glial aquaporins in rat retina. Neurosci Lett 2007; 421:132-6. [PMID: 17566653].

20. Qin Y, Fan J, Ye X, Xu G, Liu W, Da C. High salt loading alters the expression and localization of glial aquaporins in rat retina. Exp Eye Res 2009; 89:88-94. [PMID: 19268466].

21. Qin Y, Xu G, Fan J, Witt RE, Da C. High-salt loading exacerbates increased retinal content of aquaporins AQP1 and AQP4 in rats with diabetic retinopathy. Exp Eye Res 2009; 89:741-7. [PMID: 19596320].

22. Ferri D, Mazzone A, Liquori GE, Cassano G, Svelto M, Calamita G. Ontogeny, distribution, and possible functional implications of an unusual aquaporin, AQP8, in mouse liver. Hepatology 2003; 38:947-57. [PMID: 14512882].

23. Calamita G, Ferri D, Gena P, Liquori GE, Cavalier A, Thomas D, Svelto M. The inner mitochondrial membrane has aquaporin-8 water channels and is highly permeable to water. J Biol Chem 2005; 280:17149-53. [PMID: 15749715].

24. Ikaga R, Namekata I, Kotiadis VN, Ogawa H, Duchen MR, Tanaka H, Iida-Tanaka N. Knockdown of aquaporin-8 induces mitochondrial dysfunction in 3T3–L1 cells. Biochem Biophys Rep 2015; 4:187-95. [PMID: 29124204].

25. Gradilone SA, Carreras FI, Lehmann GL, Marinelli RA. Phosphoinositide 3-kinase is involved in the glucagon-induced translocation of aquaporin-8 to hepatocyte plasma membrane. Biol Cell 2005; 97:831-6. [PMID: 15859947].

26. Bertolotti M, Bestetti S, García-Manteiga JM, Medraño-Fernandez I, Dal Mas A, Malosio ML, Sitia R. Tyrosine kinase signal modulation: A matter of H_2O_2 membrane permeability? Antioxid Redox Signal 2013; 19:1447-51. [PMID: 23541115].

27. Vieceli Dalla Sega F, Zambonin L, Fiorentini D, Rizzo B, Caliceti C, Landi L, Hrelia S, Prata C. Specific aquaporins facilitate Nox-produced hydrogen peroxide transport through plasma membrane in leukaemia cells. Biochim Biophys Acta 2014; 1843:806-14. [PMID: 24440277].

28. Bienert GP, Møller AL, Kristiansen KA, Schulz A, Møller IM, Schjoerring JK, Jahn TP. Specific aquaporins facilitate the diffusion of hydrogen peroxide across membranes. J Biol Chem 2007; 282:1183-92. [PMID: 17105724].

29. Marchissio MJ, Francés DE, Carnovale CE, Marinelli RA. Mitochondrial aquaporin-8 knockdown in human hepatoma HepG2 cells causes ROS-induced mitochondrial depolarization and loss of viability. Toxicol Appl Pharmacol 2012; 264:246-54. [PMID: 22910329].

30. Liu K, Nagase H, Huang CG, Calamita G, Agre P. Purification and functional characterization of aquaporin-8. Biol Cell 2006; 98:153-61. [PMID: 15948717].

31. Saparov SM, Liu K, Agre P, Pohl P. Fast and selective ammonia transport by aquaporin-8. J Biol Chem 2007; 282:5296-301. [PMID: 17189259].

32. Hayashi R, Hayashi S, Sakai M, Arai K, Chikuda M, Machida S. Gender differences in mRNA expression of aquaporin 8 and glutathione peroxidase in cataractous lens following intake of an antioxidant supplement. Exp Eye Res 2018; 168:28-32. [PMID: 29317238].

33. Chen R, Hollborn M, Grosche A, Reichenbach A, Wiedemann P, Bringmann A, Kohen L. Effects of the vegetable polyphenols epigallocatechin-3-gallate, luteolin, apigenin, myricetin, quercetin, and cyanidin in retinal pigment epithelial cells. Mol Vis 2014; 20:242-58. [PMID: 24623967].

34. An WG, Kanekal M, Simon MC, Maltepe E, Blagosklonny MV, Neckers LM. Stabilization of wild-type p53 by hypoxia-inducible factor 1α. Nature 1998; 392:405-8. [PMID: 9537326].

35. Livak KJ, Schmittgen TD. Analysis of relative gene expression data using real-time quantitative PCR and the $2^{-\Delta\Delta CT}$ method. Methods 2001; 25:402-8. [PMID: 11846609].

36. Mulisch M, Welsch U. *Romeis Mikroskopische Technik*. Spektrum Akademischer Verlag. Heidelberg, Germany, 2010.

37. García F, Kierbel A, Larocca MC, Gradilone SA, Splinter P, LaRusso NF, Marinelli RA. The water channel aquaporin-8 is mainly intracellular in rat hepatocytes, and its plasma membrane insertion is stimulated by cyclic AMP. J Biol Chem 2001; 276:12147-52. [PMID: 11278499].

38. Crompton M, Ellinger H, Costi A. Inhibition by cyclosporin A of a Ca^{2+}-dependent pore in heart mitochondria activated by inorganic phosphate and oxidative stress. Biochem J 1988; 255:357-60. [PMID: 3196322].

39. Hollborn M, Fischer S, Wiedemann P, Bringmann A, Kohen L. Osmotic regulation of NFAT5 expression in RPE cells: The involvement of purinergic receptor signaling. Mol Vis 2017; 23:116-30. [PMID: 28356704].

40. Kleiner J, Hollborn M, Wiedemann P, Bringmann A. Activator protein-1 contributes to the NaCl-induced expression of VEGF and PlGF in retinal pigment epithelial cells. Mol Vis 2018; 24:647-66. [PMID: 30310263].

41. Lee K, Lee JH, Boovanahalli SK, Jin Y, Lee M, Jin X, Kim JH, Hong YS, Lee JJ. (Aryloxyacetylamino)benzoic acid analogues: a new class of hypoxia-inducible factor-1

inhibitors. J Med Chem 2007; 50:1675-84. [PMID: 17328532].

42. Schust J, Sperl B, Hollis A, Mayer TU, Berg T. Stattic: a small-molecule inhibitor of STAT3 activation and dimerization. Chem Biol 2006; 13:1235-42. [PMID: 17114005].

43. Natarajan K, Singh S, Burke TR Jr, Grunberger D, Aggarwal BB. Caffeic acid phenethyl ester is a potent and specific inhibitor of activation of nuclear transcription factor NF-κB. Proc Natl Acad Sci USA 1996; 93:9090-5. [PMID: 8799159].

44. Cheung CY, Ko BC. NFAT5 in cellular adaptation to hypertonic stress – regulations and functional significance. J Mol Signal 2013; 8:5-[PMID: 23618372].

45. Veltmann M, Hollborn M, Reichenbach A, Wiedemann P, Kohen L, Bringmann A. Osmotic induction of angiogenic growth factor expression in human retinal pigment epithelial cells. PLoS One 2016; 11:e0147312-[PMID: 26800359].

46. Abbracchio MP, Burnstock G, Boeynaems JM, Barnard EA, Boyer JL, Kennedy C, Knight GE, Fumagalli M, Gachet C, Jacobson KA, Weisman GA. International Union of Pharmacology LVIII: update on the P2Y G protein-coupled nucleotide receptors: from molecular mechanisms and pathophysiology to therapy. Pharmacol Rev 2006; 58:281-341. [PMID: 16968944].

47. Coll RC, Robertson AA, Chae JJ, Higgins SC, Muñoz-Planillo R, Inserra MC, Vetter I, Dungan LS, Monks BG, Stutz A, Croker DE, Butler MS, Haneklaus M, Sutton CE, Núñez G, Latz E, Kastner DL, Mills KH, Masters SL, Schroder K, Cooper MA, O'Neill LA. A small-molecule inhibitor of the NLRP3 inflammasome for the treatment of inflammatory diseases. Nat Med 2015; 21:248-55. [PMID: 25686105].

48. Pasantes-Morales H. Channels and volume changes in the life and death of the cell. Mol Pharmacol 2016; 90:358-70. [PMID: 27358231].

49. Babenko AP, Aguilar-Bryan L, Bryan J. A view of sur/KIR6.x, K_{ATP} channels. Annu Rev Physiol 1998; 60:667-87. [PMID: 9558481].

50. Ettaiche M, Heurteaux C, Blondeau N, Borsotto M, Tinel N, Lazdunski M. ATP-sensitive potassium channels (K_{ATP}) in retina: A key role for delayed ischemic tolerance. Brain Res 2001; 890:118-29. [PMID: 11164774].

51. Njie-Mbye YF, Kulkarni M, Opere CA, Ohia SE. Mechanism of action of hydrogen sulfide on cyclic AMP formation in rat retinal pigment epithelial cells. Exp Eye Res 2012; 98:16-22. [PMID: 22445555].

52. Seino S. ATP-sensitive potassium channels: A model of heteromultimeric potassium channel/receptor assemblies. Annu Rev Physiol 1999; 61:337-62. [PMID: 10099692].

53. Chen M, Dong Y, Simard JM. Functional coupling between sulfonylurea receptor type 1 and a nonselective cation channel in reactive astrocytes from adult rat brain. J Neurosci 2003; 23:8568-77. [PMID: 13679426].

54. Hsyu PH, Gisclon LG, Hui AC, Giacomini KM. Interactions of organic anions with the organic cation transporter in renal BBMV. Am J Physiol 1988; 254:F56-61. [PMID: 2962517].

55. Lamkanfi M, Mueller JL, Vitari AC, Misaghi S, Fedorova A, Deshayes K, Lee WP, Hoffman HM, Dixit VM. Glyburide inhibits the cryopyrin/Nalp3 inflammasome. J Cell Biol 2009; 187:61-70. [PMID: 19805629].

56. Zarsoso M, Reiser M, Noujaim SF. Molecular regulation of cardiac inward rectifier potassium channels by pharmacologic agents. In: Zipes DP, Jalife J, Stevenson WG (eds) *Cardiac Electrophysiology: From Cell to Bedside, 7th Ed.* Elsevier, Philadelphia, PA, 2018, pp 122–127.

57. Jellinck PH, Monder C, McEwen BS, Sakai RR. Differential inhibition of 11β-hydroxysteroid dehydrogenase by carbenoxolone in rat brain regions and peripheral tissues. J Steroid Biochem Mol Biol 1993; 46:209-13. [PMID: 8664169].

58. Bruzzone R, Barbe MT, Jacob NJ, Monyer H. Pharmacological properties of homomeric and heteromeric pannexin hemichannels expressed in *Xenopus* oocytes. J Neurochem 2005; 92:1033-43. [PMID: 15715654].

59. Burg MB, Ferraris JD, Dmitrieva NI. Cellular response to hyperosmotic stresses. Physiol Rev 2007; 87:1441-74. [PMID: 17928589].

60. Arsenijevic T, Vujovic A, Libert F, Op de Beeck A, Hébrant A, Janssens S, Grégoire F, Lefort A, Bolaky N, Perret J, Caspers L, Willermain F, Delporte C. Hyperosmotic stress induces cell cycle arrest in retinal pigmented epithelial cells. Cell Death Dis 2013; 4:e662-[PMID: 23744362].

61. Winges A, Garcia TB, Prager P, Wiedemann P, Kohen L, Bringmann A, Hollborn M. Osmotic expression of aldose reductase in retinal pigment epithelial cells: Involvement of NFAT5. Graefes Arch Clin Exp Ophthalmol 2016; 254:2387-400. [PMID: 27628063].

62. Medraño-Fernandez I, Bestetti S, Bertolotti M, Bienert GP, Bottino C, Laforenza U, Rubartelli A, Sitia R. Stress regulates aquaporin-8 permeability to impact cell growth and survival. Antioxid Redox Signal 2016; 24:1031-44. [PMID: 26972385].

63. Witmer AN, Vrensen GF, Van Noorden CJ, Schlingemann RO. Vascular endothelial growth factors and angiogenesis in eye disease. Prog Retin Eye Res 2003; 22:1-29. [PMID: 12597922].

64. Lambert IH, Pedersen SF, Poulsen KA. Activation of PLA_2 isoforms by cell swelling and ischaemia/hypoxia. Acta Physiol (Oxf) 2006; 187:75-85. [PMID: 16734744].

65. Chen M, Simard JM. Cell swelling and a nonselective cation channel regulated by internal Ca^{2+} and ATP in native reactive astrocytes from adult rat brain. J Neurosci 2001; 21:6512-21. [PMID: 11517240].

66. Ashcroft FM. ATP-sensitive potassium channelopathies: focus on insulin secretion. J Clin Invest 2005; 115:2047-57. [PMID: 16075046].

67. Garlid KD, Paucek P, Yarov-Yarovoy V, Murray HN, Darbenzio RB, D'Alonzo AJ, Lodge NJ, Smith MA, Grover GJ. Cardioprotective effect of diazoxide and its interaction with mitochondrial ATP-sensitive K^+ channels. Possible

mechanism of cardioprotection. Circ Res 1997; 81:1072-82. [PMID: 9400389].

68. Wojtovich AP, Nadtochiy SM, Brookes PS, Nehrke K. Ischemic preconditioning: The role of mitochondria and aging. Exp Gerontol 2012; 47:1-7. [PMID: 22100642].

69. Prager P, Hollborn M, Steffen A, Wiedemann P, Kohen L, Bringmann A. High salt-induced priming of retinal pigment epithelial cells for NLRP3 inflammasome activation: Contribution of $P2Y_1$ receptor signaling. PLoS One 2016; 11:e0165653-[PMID: 27788256].

70. Jian Z, Ding S, Deng H, Wang J, Yi W, Wang L, Zhu S, Gu L, Xiong X. Probenecid protects against oxygen-glucose deprivation injury in primary astrocytes by regulating inflammasome activity. Brain Res 2016; 1643:123-9. [PMID: 27154322].

71. Wu Q, Yang ZF, Wang KJ, Feng XY, Lv ZJ, Li Y, Jian ZX. AQP8 inhibits colorectal cancer growth and metastasis by down-regulating PI3K/AKT signaling and PCDH7 expression. Am J Cancer Res 2018; 8:266-79. [PMID: 29511597].

72. Dong R, Tao S, Liu Z, Zheng W, Yu D. Down-regulation of AQP8 suppresses glioma cells growth and invasion/migration via cell cycle pathway. Int J Clin Exp Pathol 2016; 9:1240-8. .

73. Maeno E, Ishizaki Y, Kanaseki T, Hazama A, Okada Y. Normotonic cell shrinkage because of disordered volume regulation is an early prerequisite to apoptosis. Proc Natl Acad Sci USA 2000; 97:9487-92. [PMID: 10900263].

74. Jablonski EM, Mattocks MA, Sokolov E, Koniaris LG, Hughes FM Jr, Fausto N, Pierce RH, McKillop IH. Decreased aquaporin expression leads to increased resistance to apoptosis in hepatocellular carcinoma. Cancer Lett 2007; 250:36-46. [PMID: 17084522].

75. Mao H, Seo SJ, Biswal MR, Li H, Conners M, Nandyala A, Jones K, Le YZ, Lewin AS. Mitochondrial oxidative stress in the retinal pigment epithelium leads to localized retinal degeneration. Invest Ophthalmol Vis Sci 2014; 55:4613-27. [PMID: 24985474].

76. Fraser-Bell S, Kaines A, Hykin PG. Update on treatments for diabetic macular edema. Curr Opin Ophthalmol 2008; 19:185-9. [PMID: 18408491].

77. Zheng Z, Chen H, Ke G, Fan Y, Zou H, Sun X, Gu Q, Xu X, Ho PC. Protective effect of perindopril on diabetic retinopathy is associated with decreased vascular endothelial growth factor-to-pigment epithelium-derived factor ratio: Involvement of a mitochondria-reactive oxygen species pathway. Diabetes 2009; 58:954-64. [PMID: 19188429].

78. Markovets AM, Fursova AZ, Kolosova NG. Therapeutic action of the mitochondria-targeted antioxidant SkQ1 on retinopathy in OXYS rats linked with improvement of VEGF and PEDF gene expression. PLoS One 2011; 6:e21682-[PMID: 21750722].

79. Reichard A, Asosingh K. The role of mitochondria in angiogenesis. Mol Biol Rep 2019; 46:1393-400. [PMID: 30460535].

80. Wright GL, Maroulakou IG, Eldridge J, Liby TL, Sridharan V, Tsichlis PN, Muise-Helmericks RC. VEGF stimulation of mitochondrial biogenesis: Requirement of AKT3 kinase. FASEB J 2008; 22:3264-75. [PMID: 18524868].

81. Guo D, Wang Q, Li C, Wang Y, Chen X. VEGF stimulated the angiogenesis by promoting the mitochondrial functions. Oncotarget 2017; 8:77020-7. [PMID: 29100366].

82. Kleinewietfeld M, Manzel A, Titze J, Kvakan H, Yosef N, Linker RA, Muller DN, Hafler DA. Sodium chloride drives autoimmune disease by the induction of pathogenic T_H17 cells. Nature 2013; 496:518-22. [PMID: 23467095].

83. Wu C, Yosef N, Thalhamer T, Zhu C, Xiao S, Kishi Y, Regev A, Kuchroo VK. Induction of pathogenic T_H17 cells by inducible salt-sensing kinase SGK1. Nature 2013; 496:513-7. [PMID: 23467085].

84. Go WY, Liu X, Roti MA, Liu F, Ho SN. NFAT5/TonEBP mutant mice define osmotic stress as a critical feature of the lymphoid microenvironment. Proc Natl Acad Sci USA 2004; 101:10673-8. [PMID: 15247420].

85. Machnik A, Neuhofer W, Jantsch J, Dahlmann A, Tammela T, Machura K, Park JK, Beck FX, Müller DN, Derer W, Goss J, Ziomber A, Dietsch P, Wagner H, van Rooijen N, Kurtz A, Hilgers KF, Alitalo K, Eckardt KU, Luft FC, Kerjaschki D, Titze J. Macrophages regulate salt-dependent volume and blood pressure by a vascular endothelial growth factor-C-dependent buffering mechanism. Nat Med 2009; 15:545-52. [PMID: 19412173].

Articles are provided courtesy of Emory University and the Zhongshan Ophthalmic Center, Sun Yat-sen University, P.R. China. The print version of this article was created on 30 December 2020. This reflects all typographical corrections and errata to the article through that date. Details of any changes may be found in the online version of the article.